



HAL
open science

Functionalised Terpyridines and Their Metal Complexes-Solid-State Interactions

Young Hoon Lee, Jee Young Kim, Sotaro Kusumoto, Hitomi Ohmagari, Miki Hasegawa, Pierre Thuéry, Jack Harrowfield, Shinya Hayami, Yang Kim

► **To cite this version:**

Young Hoon Lee, Jee Young Kim, Sotaro Kusumoto, Hitomi Ohmagari, Miki Hasegawa, et al.. Functionalised Terpyridines and Their Metal Complexes-Solid-State Interactions. *Chemistry*, 2021, 3 (1), pp.199-227. 10.3390/chemistry3010016 . cea-03134426

HAL Id: cea-03134426

<https://cea.hal.science/cea-03134426>

Submitted on 8 Feb 2021

HAL is a multi-disciplinary open access archive for the deposit and dissemination of scientific research documents, whether they are published or not. The documents may come from teaching and research institutions in France or abroad, or from public or private research centers.

L'archive ouverte pluridisciplinaire **HAL**, est destinée au dépôt et à la diffusion de documents scientifiques de niveau recherche, publiés ou non, émanant des établissements d'enseignement et de recherche français ou étrangers, des laboratoires publics ou privés.



Distributed under a Creative Commons Attribution 4.0 International License

Article

Functionalised Terpyridines and Their Metal Complexes—Solid-State Interactions †

Young Hoon Lee ¹, Jee Young Kim ², Sotaro Kusumoto ³, Hitomi Ohmagari ⁴, Miki Hasegawa ⁴, Pierre Thuéry ⁵, Jack Harrowfield ^{6,*}, Shinya Hayami ³ and Yang Kim ³

¹ Department of Chemistry, University of Ulsan, Ulsan 44610, Korea; dasis75@daum.net

² Department of Chemistry & Advanced Materials, Kosin University, 194 Wachiro, Yongdo-Gu, Busan 49104, Korea; pinkjy0117@hanmail.net

³ Department of Chemistry, Graduate School of Science and Technology, Kumamoto University, 2-39-1 Kurokami, Chuo-ku, Kumamoto 860-8555, Japan; 185d9042@st.kumamoto-u.ac.jp (S.K.); hayami@kumamoto-u.ac.jp (S.H.); ykim@kumamoto-u.ac.jp (Y.K.)

⁴ Department of Chemistry & Biological Science, College of Science & Engineering, Aoyama Gakuin University, Sagami-hara, Kanagawa 252-5258, Japan; ohmagari@chem.aoyama.ac.jp (H.O.); hasemiki@chem.aoyama.ac.jp (M.H.)

⁵ Université Paris–Saclay, CEA, CNRS, NIMBE, 91191 Gif-sur-Yvette, France; pierre.thuery@cea.fr

⁶ ISIS, Université de Strasbourg, 8 allée Gaspard Monge, 67083 Strasbourg, France

* Correspondence: harrowfield@unistra.fr; Tel.: +33-03-6885-5165

† Dedicated to Professor Christoph Janiak in recognition of his seminal contributions to the study of weak interactions in crystalline coordination complexes.

Citation: Lee, Y.H.; Kim, J.Y.; Kusumoto, S.; Ohmagari, H.; Hasegawa, M.; Thuéry, P.; Harrowfield, J.; Hayami, S.; Kim, Y. Functionalised Terpyridines and Their Metal Complexes—Solid-State Interactions. *Chemistry* **2021**, *3*, 199–227. <https://doi.org/10.3390/chemistry3010016>

Received: 12 January 2021

Accepted: 27 January 2021

Published: 5 February 2021

Publisher's Note: MDPI stays neutral with regard to jurisdictional claims in published maps and institutional affiliations.



Copyright: © 2021 by the authors. Licensee MDPI, Basel, Switzerland. This article is an open access article distributed under the terms and conditions of the Creative Commons Attribution (CC BY) license (<http://creativecommons.org/licenses/by/4.0/>).

Abstract: Analysis of the weak interactions within the crystal structures of 33 complexes of various 4'-aromatic derivatives of 2,2':6',2''-terpyridine (**tpy**) shows that interactions that exceed dispersion are dominated, as expected, by cation–anion contacts but are associated with both ligand–ligand and ligand–solvent contacts, sometimes multicentred, in generally complicated arrays, probably largely determined by dispersion interactions between stacked aromatic units. With V(V) as the coordinating cation, there is evidence that the polarisation of the ligand results in an interaction exceeding dispersion at a carbon bound to nitrogen with oxygen or fluorine, an interaction unseen in the structures of M(II) (M = Fe, Co, Ni, Cu, Zn, Ru and Cd) complexes, except when 1,2,3-trimethoxyphenyl substituents are present in the 4'-**tpy**.

Keywords: terpyridines; metal complexes; crystal structures; Hirshfeld surfaces; weak interactions

1. Introduction

Ligands based on the 2,2':6',2''-terpyridine (**tpy**) substructure have been employed in an extraordinary variety of studies concerning their metal-ion coordination chemistry [1–7]. Much of this chemistry has concerned condensed phases—crystals, liquid crystals, monolayers on surfaces, intercalation complexes, and films—where interactions between complex ion units and between them and their environment can be particularly important, as is well-known for 2,2':6',2''-terpyridine itself [8]. The postulate of the “terpyridine embrace” [9–12] as a means of rationalising the forms of the lattices of many crystalline terpyridine complexes provides a long-known example of the recognition of this fact. This form of supposed aromatic–aromatic interaction, however, is known not to be universally operative for such complexes [11,13,14], and more importantly, it is well recognised that terms, such as “ π -stacking” and “ π - π interactions” (as well as “OFF” = offset face-to-face and “EF” = edge-to-face aromatic interactions), widely applied to the description of putative interactions between aromatic entities [15–17] can be rather eclectically interpreted and that there may be infrequent reason to attribute special significance to the association of small aromatic systems beyond the recognition of dispersion interactions

[18–24]. An even broader issue is that of whether intermolecular interactions should be considered parallel to molecular bonding in being the result of the combination of proximal two-centre interactions [25–27]. Thus, the dissection of a crystal lattice in terms of atom–atom “contacts”, which may or may not be indicative of attractive, labile interactions, is not a straightforward task [25–32], so in the work now reported, we crystallographically characterised a series of complexes of related 4′ derivatives of 2,2′:6′,2′′-terpyridine (Figure 1) in the hope that systematic structural variations might facilitate the identification of major interactions. To assess the interactions within the lattices, we employed the calculation of Hirshfeld surfaces [29] using the program CrystalExplorer [30]. This work is a complement to other structural studies of functionalised terpyridines and their complexes that we have reported [14,33–37] and provides results to be integrated with the present and with the extant literature in general. The ultimate objective, in general, is, of course, to use such information in the design and synthesis of functional materials [38].

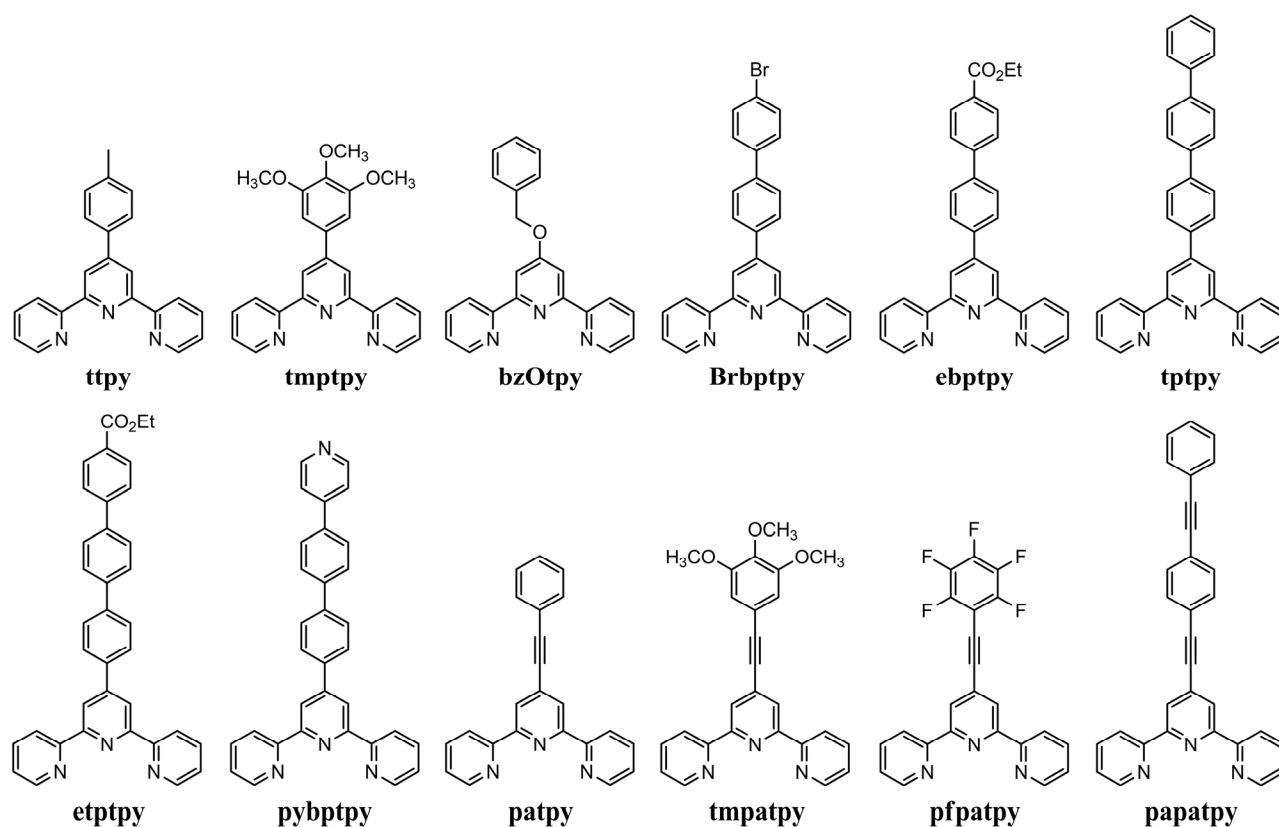


Figure 1. 4′-substituted derivatives of 2,2′:6′,2′′-terpyridine studied in the present work.

2. Experimental Section

2.1. General

Dichloromethane and acetonitrile (spectrophotometric grade) for the measurement of electronic absorption and emission spectra were purchased from Merck (Seoul, S. Korea). Other organic solvents were purchased from Aldrich (Basel, Switzerland). Reagents were purchased from Wako (Osaka, Japan) (pyridin-4-yl-4-boronic acid and 4-(ethoxycarbonyl)phenylboronic acid), Tokyo Chemical Industry (Tokyo, Japan) (benzylbromide, 2,2′:6′,2′′-terpyridine (**tpy**), 1-bromo-4-iodobenzene, Pd(PPh₃)₄ and 1,2,3,4,5-pentafluoro-6-iodobenzene), Alfa Aesar (Sulzbach, Germany) ((trimethylsilyl)acetylene and 1-ethynylbenzene) and Aldrich (Basel, Switzerland) (diisopropylamine, CuI, ZnCl₂, CdCl₂, RuCl₃·xH₂O, Co(BF₄)₂·6H₂O, Fe(ClO₄)₂·H₂O,

Ni(ClO₄)₂·6H₂O, Cu(ClO₄)₂·6H₂O, Zn(ClO₄)₂·6H₂O, Cd(ClO₄)₂·H₂O and K₂CO₃) and used without further purification. Elemental analyses (C, H and N) were carried out at the Instrumental Analysis Centre of Kumamoto University, Japan. ¹H-NMR spectra were recorded with JEOL 500-ECX (500 MHz) and Bruker 300 AM spectrometers (300.13 MHz) in deuterated solvents using TMS as an internal reference. Electronic absorption spectra were recorded on SCINCO S-2100 and Varian Cary 100 spectrophotometers. Fluorescence spectra were recorded on Perkin Elmer LS55 and HORIBA FluoroMax-4P instruments. 1-bromo-4-(2-phenylethynyl)benzene [39], 2,2':6',2''-terpyridine-4'-ol [40], 2,6-bis(pyridin-2-yl)pyridin-4-yl trifluoromethanesulfonate [41], 2-(4-ethynyl-6-(pyridin-2-yl)pyridin-2-yl)pyridine (4'-ethynyl-2,2':6',2''-terpyridine) [42], 4'-(biphenyl-4-yl)-2,2':6',2''-terpyridine (**btpy**) [43], 4'-(tolyl)-2,2':6',2''-terpyridine (**ttpy**) [44], 4'-(3,4,5-trimethoxy-phenyl)-2,2':6',2''-terpyridine (**tmtpy**) [45], 2-(4-(2-phenylethynyl)-6-(pyridin-2-yl)pyridin-2-yl)pyridine (**patpy**) [46–48], 4'-((ethoxycarbonyl)biphenyl-4-yl)-2,2':6',2''-terpyridine (**ebtpy**) [49], 4'-((ethoxycarbonyl)terphenyl-4-yl)-2,2':6',2''-terpyridine (**ettpyb**) [33], 4'-(benzyloxy)-2,2':6',2''-terpyridine, (**bzOtpy**) [33], 4'-(pentafluorophenyl)-2,2':6',2''-terpyridine (**pfpatpy**) [33], 4'-terphenyl-2,2':6',2''-terpyridine (**tpy**) [34], 4'-(4'-pyridin-4-yl-biphenyl-4-yl)-2,2':6',2''-terpyridine (**pybtpy**) [35], 4'-(4-bromobiphenyl-4-yl)-2,2':6',2''-terpyridine (**Brbtpy**) [36], 2-(4-(2-(3,4,5-trimethoxyphenyl)ethynyl)-6-(pyridin-2-yl)pyridin-2-yl)pyridine (**tmtpatpy**) [37] and [Ru(**tpy**)Cl₃] [50] were prepared by literature methods. The synthesis of the ligand 4'-(4'''-(ethynylphenyl)phenylethynyl)-2,2':6',2''-terpyridine (**papatpy**) is described below along with that of its complexes.

2.2. Synthesis

CAUTION! Most of the complexes described were isolated as perchlorate salts and are thus potential explosives. Although no difficulties were encountered, such materials should always be prepared in the minimum possible quantities.

2.2.1. Vanadium(V) Complex of 4'-(Biphenyl)-2,2':6',2''-terpyridine, Btpy

(1) [VO₂(**btpy**)]ClO₄: **Btpy** (120 mg, 0.3 mmol) was dissolved in CHCl₃/CH₃OH (20 mL, 1:1, *v/v*) and VOSO₄·3H₂O (65 mg, 0.3 mmol) in methanol (10 mL), added with stirring. Under exposure to a normal atmosphere, the initially blue solution slowly changed colour to yellow–green over several hours, after which NaClO₄ (0.4 g) was dissolved in it, and the solution was allowed to slowly evaporate under ambient temperature to produce yellow crystals suitable for an X-ray diffraction study (yield: 90 mg, 53%). Anal. calc. for C₂₇H₁₉ClN₃O₆V: C, 57.11; H, 3.37; N, 7.40. Found: C, 56.88; H, 3.50; N, 7.26%. CCDC number, 2055133.

2.2.2. Complexes of 4'-Terphenyl-2,2':6',2''-terpyridine, Ttpy (and Mixed Complexes with 2,2':6',2''-Terpyridine)

(2) [Fe(**tpy**)₂](ClO₄)₂·CH₃OH: Fe(ClO₄)₂·6H₂O (9.0 mg, 0.025 mmol) in DMF (5 mL) was added to a solution of **tpy** (30 mg, 0.065 mmol) in hot DMF (5 mL). After stirring the solution for 2 h at 100 °C, the solvent was removed under reduced pressure. The deep purple residue was washed with methanol and chloroform, and dried at ambient temperature (yield: 25 mg, quantitative). Anal. calc. for C₆₇H₄₉Cl₂N₆FeO₉: C, 66.57; H, 4.09; N, 6.95. Found: C, 66.52; H, 4.07; N, 6.98%. ¹H-NMR (300 MHz) in CD₃CN: δ 9.26 (s, 4H), 8.66 (d, *J* = 8.0 Hz, 4H), 8.46 (d, *J* = 8.0 Hz, 4H), 8.17 (d, *J* = 8.0 Hz, 4H), 7.99 (d, *J* = 8.0 Hz, 4H), 7.94 (t, *J* = 8.5 Hz, 4H), 7.88 (d, *J* = 8.0 Hz, 4H), 7.78 (d, *J* = 7.5 Hz, 4H), 7.55 (t, *J* = 7.5 Hz, 4H), 7.45 (t, *J* = 7.5 Hz, 2H), 7.22 (d, *J* = 5.5 Hz, 4H), 7.11 (t, *J* = 7.0 Hz, 4H). The vapour diffusion of methanol into a solution of the complex in a minimum volume of DMF produced purple crystals suitable for X-ray diffraction studies. CCDC number, 2055134.

(3) [Ni(tptpy)₂](ClO₄)₂·CH₃OH: Ni(ClO₄)₂·6H₂O (8.0 mg, 0.022 mmol) in methanol (5 mL) was added to a solution of **tptpy** (20 mg, 0.043 mmol) in CHCl₃/CH₃OH (6 mL, 1:1, *v/v*). After stirring the solution for 1 h at 60 °C, the solvent was removed under reduced pressure. The yellow residue was washed with methanol and chloroform, and then dried at ambient temperature (yield: 20 mg, 91%). Anal. calc. for C₆₇H₄₉Cl₂N₆NiO₉: C, 66.41; H, 4.08; N, 6.94. Found: C, 66.50; H, 4.02; N, 7.01%. The vapour diffusion of methanol into a solution of the complex in a minimum volume of DMF produced yellow crystals suitable for X-ray diffraction studies. CCDC number, 2055135.

(4) [Ru(tptpy)₂](PF₆)₂·3CH₃CN: A mixture of **tptpy** (100 mg, 0.22 mmol) and RuCl₃·xH₂O (50 mg, 0.22 mmol) in ethanol (30 mL) was heated at 70 °C for 6 h to produce a turbid, reddish solution. After cooling to ambient temperature, the brown precipitate formed was collected by filtration, washed with cold ethanol and then dried under vacuum. The elemental analyses were consistent with its formulation as [Ru(tptpy)Cl₃] (yield: 80 mg). [Ru(tptpy)Cl₃] (30 mg, 0.045 mmol), **tptpy** (30 mg, 0.065 mmol) and *N*-ethylmorpholine (five drops) were added to methanol/chloroform (30 mL, 1:1, *v/v*), and the mixture was heated at 70 °C for 2 h. The resulting deep red solution was filtered through Celite to remove a small amount of purple precipitate. The filtrate was loaded on a short silica column, and the column eluted with acetonitrile/saturated aqueous KNO₃/water at 7:1:0.5, *v/v*. The major red component was collected, and methanolic NH₄PF₆ was added to the eluate to produce a red powder within 1 h. This was collected by filtration, washed with methanol and then dried under vacuum (yield: 30 mg, 50%). Anal. calc. for C₇₂H₅₅F₁₂N₉P₂Ru: C, 60.17; H, 3.86; N, 8.77. Found: C, 60.22; H, 3.83; N, 8.80%. Electronic absorption spectrum (in CH₃CN): λ_{max} (ε_{max}/M⁻¹ cm⁻¹) = 285 nm (58,900), 312 nm (75,500), 330 nm (72,300), 494 nm (32,100). ¹H-NMR (500 MHz) in CD₃CN: δ 9.08 (s, 4H), 8.69 (d, *J* = 7.5 Hz, 4H), 8.35 (d, *J* = 8.0 Hz, 4H), 8.13 (d, *J* = 8.0 Hz, 4H), 7.98 (m, 8H), 7.87 (d, *J* = 7.5 Hz, 4H), 7.54 (t, *J* = 8.0 Hz, 4H), 7.46 (m, 6H), 7.21 (t, *J* = 6.5 Hz, 4H). The slow evaporation of an acetonitrile solution of the complex at ambient temperature produced red crystals suitable for X-ray structure determination. CCDC number, 2055219.

(5) [Ru(tptpy)(tpy)](PF₆)₂·2DMF: **Ttpy** (60 mg, 0.13 mmol), [Ru(tpy)Cl₃] (50 mg, 0.11 mmol) and *N*-ethylmorpholine (five drops) were added to methanol/chloroform (30 mL, 1:1, *v/v*), and the mixture was heated at 70 °C for 2 h. The resulting deep red solution was filtered through Celite to remove a small amount of brown precipitate, and the filtrate was subjected to chromatography on silica using acetonitrile/saturated aqueous KNO₃/water at 7:1:0.5, *v/v*, as the eluant. The major red component was collected, and methanolic NH₄PF₆ was added to the eluate to produce a red precipitate, which was filtered and washed with methanol, and then dried in a vacuum (yield: 23 mg, 20%). Anal. calc. for C₅₄H₄₈F₁₂N₈O₂P₂Ru: C, 52.64; H, 3.93; N, 9.10. Found: C, 52.55; H, 3.85; N, 9.05%. IR spectrum (KBr disc, cm⁻¹): 3106, 3038, 3030 (Ar C–H), 863 (PF₆). Electronic absorption spectrum (in CH₃CN): λ_{max} (ε_{max}, M⁻¹ cm⁻¹) = 275 nm (43,700), 282 nm (43,900), 309 nm (73,900), 485 nm (24,800). ¹H-NMR (500 MHz) in CD₃CN: δ 9.06 (s, 2H), 8.75 (d, *J* = 8.0 Hz, 2H), 8.67 (d, *J* = 8.0 Hz, 2H), 8.50 (d, *J* = 8.5 Hz, 2H), 8.42 (t, *J* = 8.5 Hz, 1H), 8.33 (d, *J* = 8.0 Hz, 2H), 8.12 (d, *J* = 8.0 Hz, 2H), 7.96 (m, 7H), 7.86 (d, *J* = 8.0 Hz, 2H), 7.77 (d, *J* = 7.5 Hz, 2H), 7.54 (t, *J* = 7.5 Hz, 2H), 7.44 (d, *J* = 5.0 Hz, 2H), 7.35 (d, *J* = 5.5 Hz, 2H), 7.18 (m, 4H). Upon dissolving the complex in hot DMF and then allowing the solution to stand for one week at ambient temperature, red crystals suitable for X-ray structure determination were obtained. CCDC number, 2055220.

(6) [Ru(tptpy)(tpy)](ClO₄)₂·2DMF: [Ru(tptpy)(tpy)](PF₆)₂ (20 mg, 0.018 mmol) was dissolved in DMF (3 mL), and LiClO₄ (0.01 g) was added. The slow deposition of red crystals suitable for X-ray structure determination occurred upon leaving the solution to stand at ambient temperature. Anal. calc. for C₅₄H₄₈Cl₂N₈O₁₀Ru: C, 56.84; H, 4.24; N, 9.82. Found: C, 56.78; H, 4.27; N, 9.78%. Electronic absorption spectrum in CH₃CN: λ_{max} (ε_{max}, M⁻¹ cm⁻¹) = 274 nm (44,000), 281 nm (43,300), 308 nm (71,400), 484 nm (23,600). ¹H-NMR (500 MHz) in CD₃CN: δ 9.06 (s, 2H), 8.75 (d, *J* = 8.5 Hz, 2H), 8.67 (d, *J* = 8.0 Hz, 2H), 8.50 (d, *J* = 8.0 Hz, 2H), 8.42 (t, *J* = 8.0 Hz, 1H), 8.33 (d, *J* = 8.5 Hz, 2H), 8.12 (d, *J* = 8.0 Hz, 2H), 7.96

(m, 7H), 7.86 (d, $J = 8.0$ Hz, 2H), 7.77 (d, $J = 8.5$ Hz, 2H), 7.54 (t, $J = 7.5$ Hz, 2H), 7.44 (d, $J = 6.0$ Hz, 2H), 7.35 (d, $J = 5.0$ Hz, 2H), 7.18 (m, 4H). CCDC number, 2055221.

2.2.3. Zinc(II) Complex of 2-(4-(2-Phenylethynyl)-6-(pyridin-2-yl)pyridin-2-yl)pyridine, Patpy

(7) **[Zn(patpy)₂](ClO₄)₂ (YK758)**: Zn(ClO₄)₂·6H₂O (30 mg, 0.08 mmol) and **patpy** (50 mg, 0.15 mmol) were dissolved in acetonitrile (10 mL) and heated at 70 °C for 2 h. After cooling to ambient temperature, the solvent was removed by evaporation under reduced pressure. The colourless residue was washed with methanol and dichloromethane and dried at ambient temperature (yield: 39 mg, 53%). Anal. calc. for C₄₆H₃₀Cl₂N₆ZnO₈: C, 59.34; H, 3.25; N, 9.03. Found: C, 59.41; H, 3.32; N, 9.20%. ¹H-NMR (300 MHz) in CD₃CN: δ 8.90 (s, 4H), 8.61 (d, $J = 8.0$ Hz, 4H), 8.22 (td, $J = 7.9, 1.6$ Hz, 4H), 7.86 (m, 8H), 7.62 (m, 6H), 7.46 (dd, $J = 5.1, 0.9$ Hz, 2H), 7.43 (dd, $J = 5.1, 0.9$ Hz, 2H). The slow evaporation of an acetonitrile solution of the complex at ambient temperature provided colourless crystals suitable for X-ray diffraction studies. CCDC number, 2055222.

2.2.4. Complexes of 4'-(4''-(Ethynylphenyl)phenylethynyl)-2,2':6',2''-terpyridine, Papatpy

(8) **papatpy**: 2-(4-ethynyl-6-(pyridin-2-yl)pyridin-2-yl)pyridine (0.25 g, 0.97 mmol), 1-bromo-4-(2-phenylethynyl)benzene (0.30 g, 1.12 mmol), Pd(PPh₃)₄ (0.10 g, 0.086 mmol) and CuI (0.020 g, 0.11 mmol) were placed into a three-necked round-bottom flask under a nitrogen atmosphere. Degassed *i*-Pr₂NH/THF (30 mL, 1:1, *v/v*) was added to the mixture and heated under reflux for 12 h under nitrogen. The resultant dark brown, turbid solution was filtered, and the filter was washed with THF. The filtrate and wash solution were evaporated to dryness under reduced pressure, and then dissolved in a minimum volume of dichloromethane. Adsorption on a short silica column and elution with ethylacetate/CH₂Cl₂ at 1:4, *v/v*, produced a colourless eluate, which was evaporated under reduced pressure to produce a white powder (yield: 0.20 g). ¹H-NMR (300 MHz) in CDCl₃: δ 8.78 (dq, $J = 4.1, 0.8$ Hz, 2H), 8.69 (d, $J = 8.0$ Hz, 2H), 8.12 (s, 2H), 7.96 (td, $J = 7.8, 1.8$ Hz, 2H), 7.59 (m, 6H), 7.43 (m, 5H). Anal. calc. for C₃₁H₁₉N₃·0.5H₂O: C, 84.14; H, 4.56; N, 9.50. Found: C, 83.70; H, 4.48; N, 9.33%.

(9) **[Co(papatpy)₂](BF₄)₃·2CH₃CN**: Co(BF₄)₂·6H₂O (0.0080 g, 0.023 mmol) in DMF (5 mL) was mixed with **papatpy** (20 mg, 0.046 mmol) in DMF (10 mL). After heating this solution for 2 h at 100 °C, the solvent was removed under reduced pressure to produce a brown residue, which was washed with methanol and chloroform, and then dried at ambient temperature (yield: 20 mg, 69%). Anal. calc. for C₆₆H₄₄B₃CoF₁₂N₈: C, 62.49; H, 3.50; N, 8.83. Found: C, 62.55; H, 3.42; N, 8.90%. The vapour diffusion of diethyl ether into an acetonitrile solution of the complex provided yellow, rod-like crystals suitable for X-ray diffraction studies. The structure determination and colour of the complex showed that the oxidation of Co(II) to Co(III) had occurred during the synthesis. CCDC number, 2055223.

(10) **[Ni(papatpy)₂](ClO₄)₂·3DMF**: Ni(ClO₄)₂·6H₂O (9.0 mg, 0.025 mmol) in DMF (5 mL) was mixed with **papatpy** (20 mg, 0.046 mmol) in DMF (10 mL). After heating this solution for 2 h at 100 °C, the solvent was removed under reduced pressure to produce a yellow residue, which was washed with methanol and chloroform, and then dried at ambient temperature (yield: 20 mg, 63%). Anal. calc. for C₇₁H₅₉Cl₂N₉NiO₁₁: C, 63.45; H, 4.43; N, 9.38. Found: C, 63.56; H, 4.42; N, 9.42%. The slow evaporation of a DMF solution of the complex at ambient temperature led to the deposition of yellow, rod-like crystals suitable for X-ray diffraction studies. CCDC number, 2055137.

(11) **[Cu(papatpy)₂](ClO₄)₂·2CH₃CN·0.5H₂O**: Cu(ClO₄)₂·6H₂O (9.0 mg, 0.024 mmol) in DMF (5 mL) was mixed with **papatpy** (20 mg, 0.046 mmol) in DMF (10 mL). After heating this solution for 2 h at 100 °C, the solvent was removed under reduced pressure. The green residue was washed with methanol and chloroform, and then dried at ambient temperature (yield: 19 mg, 66%). Anal. calc. for C₁₃₂H₉₀Cl₄Cu₂N₁₆O₁₇: C, 64.95; H, 3.72; N, 9.18. Found: C, 65.06; H, 3.52; N, 9.22%. The slow evaporation of an acetonitrile solution

of the complex at ambient temperature led to the deposition of green, block-like crystals suitable for X-ray diffraction studies. CCDC number, 2055138.

(12) [Zn(papatpy)₂](ClO₄)₂·3DMF: Zn(ClO₄)₂·6H₂O (9.0 mg, 0.023 mmol) in DMF (5 mL) was mixed with **papatpy** (20 mg, 0.046 mmol) in DMF (10 mL). After heating this solution for 2 h at 100 °C, the solvent was removed under reduced pressure to produce a colourless residue, which was washed with methanol and chloroform, and then dried at ambient temperature (yield: 21 mg, 68%). Anal. calc. for C₇₁H₅₉Cl₂N₉ZnO₁₁: C, 63.14; H, 4.40; N, 9.33. Found: C, 63.10; H, 4.45; N, 9.30%. ¹H-NMR (300 MHz; CD₃CN): δ = 8.90 (s, 4H), 8.60 (d, *J* = 9.0 Hz, 4H), 8.23 (td, *J* = 7.8, 1.5 Hz, 4H), 7.86 (m, 8H), 7.76 (d, *J* = 8.5 Hz, 4H), 7.65 (m, 4H), 7.50 (m, 6H), 7.47 (dd, *J* = 5.1, 0.9 Hz, 2H), 7.43 (dd, *J* = 5.1, 1.0 Hz, 2H). The slow evaporation of a DMF solution of the complex at ambient temperature led to the deposition of colourless, rod-like crystals suitable for X-ray diffraction studies. CCDC number, 2055139.

(13) [Ru(papatpy)₂](PF₆)₂: A mixture of **papatpy** (40 mg, 0.092 mmol) and RuCl₃·xH₂O (0.020 g) in ethanol (30 mL) was heated at 70 °C for 5 h to produce a turbid, reddish-purple solution. The precipitate formed after cooling to ambient temperature was collected and washed on a filter with cold ethanol to produce a brown powder, taken to be [Ru(papatpy)Cl₃]. [Ru(papatpy)Cl₃] (25 mg, 0.039 mmol), **papatpy** (20 mg, 0.046 mmol) and *N*-ethylmorpholine (five drops) in CH₃OH/CHCl₃ (40 mL, 3:1, *v/v*) were heated at 70 °C for 4 h. The resultant deep red solution was filtered through Celite to remove some insoluble purple material, and the solvent was evaporated off under reduced pressure. The dark red residue was dissolved in a minimum volume of acetonitrile and subjected to chromatography on a short silica column using acetonitrile/saturated aqueous KNO₃/water at 7:1:0.5, *v/v*, as the eluent. The major red component was collected, and methanolic NH₄PF₆ was added to this eluate. After 1 h, the red precipitate was filtered off, washed with methanol and then dried under vacuum (yield: 23 mg, 47%). Anal. calc. for C₆₂H₃₈F₁₂N₆P₂Ru: C, 59.19; H, 3.04; N, 6.68. Found: C, 59.10; H, 3.12; N, 6.72%. ¹H-NMR (300 MHz) in CD₃CN: δ 8.92 (s, 4H), 8.55 (dq, *J* = 8.1, 0.4 Hz, 4H), 8.01 (td, *J* = 7.8, 1.5 Hz, 4H), 7.85 (d, *J* = 8.6 Hz, 4H), 7.76 (d, *J* = 8.6 Hz, 4H), 7.66 (m, 4H), 7.50 (m, 6H), 7.45 (dq, *J* = 5.5, 0.6 Hz, 4H), 7.25 (dd, *J* = 5.6, 1.3 Hz, 2H), 7.22 (dd, *J* = 5.6, 1.3 Hz, 2H). The slow evaporation of a solution of the complex in CH₃CN at ambient temperature produced red crystals suitable for X-ray structure determination. CCDC number, 2055140.

(14) [Ru(papatpy)(tpy)](PF₆)₂·3CH₃CN: [Ru(tpy)Cl₃] (50 mg, 0.11 mmol) and **papatpy** (60 mg, 0.14 mmol) were dissolved in methanol/chloroform (30 mL, 1:1, *v/v*), and *N*-ethylmorpholine (five drops) was added. The mixture was heated under reflux for 2 h and filtered through Celite to remove a small amount of brown precipitate. The deep red filtrate was chromatographed with a short silica-gel column using a mixed eluent (acetonitrile/saturated aqueous KNO₃/water at 7:1:0.5, *v/v*). The major red band was collected, and excess methanolic NH₄PF₆ was added. The red precipitate obtained was filtered, washed with methanol and dried under vacuum (yield: 28 mg, 22%). The product was dissolved in CH₃CN and left for one week at room temperature to afford red crystals suitable for X-ray diffraction studies. Anal. calc. for C₅₂H₃₉F₁₂N₉P₂Ru: C, 52.89; H, 3.33; N, 10.67. Found: C, 52.95; H, 3.20; N, 10.81%. ¹H-NMR (300 MHz, CD₃CN): δ = 8.90 (s, 2H), 8.78 (d, *J* = 8.2 Hz, 2H), 8.54–8.50 (m, 4H), 8.45 (t, *J* = 8.2 Hz, 1H), 7.94 (qd, *J* = 7.9, 1.5 Hz, 4H), 7.83 (d, *J* = 8.0 Hz, 2H), 7.74 (d, *J* = 8.5 Hz, 2H), 7.65–7.62 (m, 2H), 7.50–7.47 (m, 3H), 7.42–7.37 (m, 4H), 7.24–7.16 (m, 4H). CCDC number, 2055141.

(15) [Cd(papatpy)₂](ClO₄)₂·2CH₃CN·H₂O: Cd(ClO₄)₂·H₂O (8.0 mg, 0.026 mmol) in DMF (5 mL) was mixed with **papatpy** (20 mg, 0.046 mmol) in DMF (10 mL). After heating this solution for 2 h at 100 °C, the solvent was removed under reduced pressure. The colourless residue was washed with methanol and chloroform, and then dried at ambient temperature (yield: 18 mg, 55%). Anal. calc. for C₆₆H₄₆Cl₂N₈CdO₉: C, 62.01; H, 3.63; N, 8.76. Found: C, 61.97; H, 3.55; N, 8.82%. ¹H-NMR (300 MHz) in CD₃CN: δ 8.85 (s, 4H), 8.64 (d, *J* = 8.1 Hz, 4H), 8.26 (td, *J* = 7.8, 1.6 Hz, 4H), 8.13 (s, 4H), 7.82 (d, *J* = 8.4 Hz, 4H), 7.75 (d, *J* = 8.4 Hz, 4H), 7.65 (m, 4H), 7.56 (d, *J* = 5.1 Hz, 2H), 7.53 (d, *J* = 5.1 Hz, 2H), 7.49 (m, 6H). The vapour diffusion of

diethyl ether into an acetonitrile solution of the complex provided colourless, rod-like crystals suitable for X-ray diffraction studies. CCDC number, 2055142.

(16) [Cd(papatpy)Cl₂] \cdot CH₂Cl₂: CdCl₂ (13 mg, 0.071 mmol) in CH₃CN/CHCl₃ (10 mL, 1:1, *v/v*) was mixed with **papatpy** (30 mg, 0.069 mmol) in chloroform (5 mL). After heating this solution at 70 °C for 2 h, the solvent was removed under reduced pressure. The colourless residue was washed with methanol and chloroform, and then dried at ambient temperature (yield: 32 mg, 64%). Anal. calc. for C₃₂H₂₁Cl₄N₃Cd: C, 54.77; H, 3.02; N, 5.99. Found: C, 54.67; H, 3.11; N, 5.88%. ¹H-NMR (300 MHz) in DMSO-*d*₆: δ 8.79 (d, *J* = 4.3 Hz, 4H), 7.78 (d, *J* = 8.1 Hz, 4H), 7.73 (d, *J* = 8.4 Hz, 4H), 7.62 (m, 3H), 7.48 (m, 4H). The slow evaporation of a solution of the complex in CH₃CN/CH₂Cl₂ (1:1, *v/v*) produced colourless, rod-like crystals suitable for X-ray diffraction studies. CCDC number, 2055224.

2.2.5. Iron(II) Complex of 4'-(Pentafluorophenylethynyl)-2,2':6',2''-terpyridine, **pfpatpy**

(17) [Fe(pfpatpy)₂](ClO₄)₂ \cdot CH₃CN \cdot H₂O: Fe(ClO₄)₂ \cdot 6H₂O (9.0 mg, 0.025 mmol) in DMF (5 mL) was added to a solution of **pfpatpy** (30 mg, 0.065 mmol) in hot DMF (5 mL). After stirring for 2 h at 100 °C, the solvent was removed under reduced pressure, and the deep purple residue was washed with CH₃OH and CHCl₃, and then dried at room temperature (yield: 25 mg, 89%). It was dissolved in DMF, and CH₃CN vapour was diffused in to produce purple crystals suitable for X-ray diffraction studies. Anal. calc. for C₄₆H₂₀Cl₂F₁₀FeN₆O₈ \cdot 0.5CH₃CN \cdot H₂O: C, 49.56; H, 2.08; N, 7.99. Found: C, 49.98; H, 1.91; N, 7.70%. (There was a partial loss of CH₃CN by comparison with the crystal.) CCDC number, 2055225.

2.2.6. Complexes of 4'-(4'-Pyridin-4-yl-biphenyl-4-yl)-2,2':6',2''-terpyridine, **pybptpy**

(18) [Ni(pybptpy)₂](ClO₄)₂ \cdot 2DMF \cdot H₂O: Ni(ClO₄)₂ \cdot 6H₂O (20 mg, 0.055 mmol) in DMF (5 mL) was added to **pybptpy** (50 mg, 0.11 mmol) in DMF (10 mL). After stirring the solution for 2 h at 100 °C, the solvent was removed under reduced pressure, and the yellow residue was washed with methanol and chloroform, and then dried at ambient temperature (yield: 54 mg, 82%). Anal. calc. for C₇₀H₆₀Cl₂N₁₀NiO₁₁: C, 62.42; H, 4.49; N, 10.40. Found: C, 62.4; H, 4.45; N, 10.21%. The vapour diffusion of methanol into a DMF solution of the complex produced yellow crystals suitable for X-ray diffraction studies. CCDC number, 2055226.

(19) [Cu(pybptpy)₂](ClO₄)₂ \cdot 3DMF \cdot H₂O: Cu(ClO₄)₂ \cdot 6H₂O (20 mg, 0.055 mmol) in DMF (5 mL) was added to **pybptpy** (50 mg, 0.11 mmol) in DMF (10 mL). After stirring the solution for 2 h at 100 °C, the solvent was removed under reduced pressure, and the green residue was washed with methanol and chloroform, and then dried at ambient temperature (yield: 58 mg, 74%). Anal. calc. for C₇₃H₆₇Cl₂CuN₁₁O₁₂: C, 61.54; H, 4.74; N, 10.81. Found: C, 61.33; H, 4.82; N, 10.88%. The vapour diffusion of methanol into a DMF solution of the complex produced green crystals suitable for X-ray diffraction studies. CCDC number, 2055227.

(20) [Zn(pybptpy)₂](ClO₄)₂ \cdot 2DMF \cdot H₂O: Zn(ClO₄)₂ \cdot 6H₂O (20 mg, 0.055 mmol) in DMF (5 mL) was added to **pybptpy** (50 mg, 0.11 mmol) in DMF (10 mL), and the solution was stirred for 2 h at 100 °C before the solvent was removed under reduced pressure. The white residue was washed with methanol and chloroform, and then dried at ambient temperature (yield: 49 mg, 63%). Anal. calc. for C₇₀H₆₀Cl₂N₁₀O₁₁Zn: C, 62.11; H, 4.47; N, 10.35. Found: C, 62.07; H, 4.55; N, 10.51%. ¹H-NMR (300 MHz) in DMSO-*d*₆: δ 9.50 (s, 4H), 9.23 (d, *J* = 8.2 Hz, 4H), 8.73 (d, *J* = 5.6 Hz, 4H), 8.63 (d, *J* = 7.8 Hz, 4H), 8.35 (t, *J* = 7.6 Hz, 4H), 8.22 (d, *J* = 8.2 Hz, 4H), 8.12 (d, *J* = 8.3 Hz, 4H), 8.05 (m, 8H), 7.86 (d, *J* = 5.8 Hz, 4H), 7.56 (t, *J* = 6.5 Hz, 4H). The vapour diffusion of methanol into a DMF solution of the complex produced colourless crystals suitable for X-ray diffraction studies. CCDC number, 2055228.

2.2.7. Complexes of 4'-(4-Bromobiphenyl-4-yl)-2,2':6',2''-terpyridine, Brbptpy

(21) **[Co(Brbptpy)₂](BF₄)₂·2CH₃CN**: Co(BF₄)₂·6H₂O (20 mg, 0.060 mmol) in dimethylformamide (DMF; 5 mL) was added to a solution of **Brbptpy** (50 mg, 0.11 mmol) in hot DMF (10 mL). After stirring for 2 h at 100 °C, the solvent was removed under reduced pressure. The brown residue was washed with methanol and dried at ambient temperature (yield: 0.048 g, 71%). Anal. calc. for C₅₈H₄₂Br₂CoF₈N₈: C, 56.03; H, 3.40; N, 9.0. Found: C, 56.18; H, 3.36; N, 8.95%. The vapour diffusion of diethyl ether into a solution of the complex in a minimum volume of acetonitrile produced brown crystals suitable for X-ray diffraction studies. CCDC number, 2055148.

(22) **[Ni(Brbptpy)₂](ClO₄)₂·DMF·H₂O**: Ni(ClO₄)₂·6H₂O (40 mg, 0.12 mmol) in methanol (10 mL) was added to a solution of **Brbptpy** (100 mg, 0.22 mmol) in CHCl₃/CH₃OH (10 mL, 1:1, *v/v*). After stirring the solution for 1 h at 60 °C, the solvent was removed under reduced pressure, and the yellow residue was washed with cold methanol and chloroform, and then dried at ambient temperature (yield: 100 mg, 68%). Anal. calc. for C₁₁₁H₇₉Br₄C₁₄N₁₃Ni₂O₁₈: C, 54.16; H, 3.2; N, 7.40. Found: C, 54.32; H, 3.30; N, 7.45%. The vapour diffusion of methanol into a solution of the complex in a minimum volume of DMF produced yellow crystals suitable for X-ray diffraction studies. CCDC number, 2055149.

(23) **[Cu(Brbptpy)₂](ClO₄)₂·2CH₃OH**: Cu(ClO₄)₂·6H₂O (45 mg, 0.12 mmol) in methanol (10 mL) was added to a solution of **Brbptpy** (100 mg, 0.22 mmol) in CHCl₃/CH₃OH (10 mL, 1:1, *v/v*). After stirring the solution for 1 h at 60 °C, the solvent was removed under reduced pressure, and the green residue was washed with cold methanol and chloroform, and then dried at ambient temperature (yield: 110 mg, 75%). Anal. calc. for C₅₆H₄₃Br₂Cl₂CuN₆O₁₀: C, 53.63; H, 3.46; N, 6.70. Found: C, 56.28; H, 3.38; N, 6.75%. The complex was dissolved in boiling methanol, and the solution was allowed to evaporate slowly at ambient temperature to provide brown crystals suitable for X-ray diffraction studies. CCDC number, 2055150.

(24) **[Ru(Brbptpy)₂](PF₆)₂·3CH₃CN**: With the substitution of **Brbptpy** for **tpptpy**, the same procedure as used with complex 4 provided red crystals (with a 51% yield) of the complex suitable for structure determination. Anal. calc. for C₆₀H₄₅Br₂F₁₂N₉P₂Ru: C, 49.95; H, 3.14; N, 8.74. Found: C, 49.35; H, 3.30; N, 8.82%. Due to the loss of the sample, an NMR spectrum was not obtained. CCDC number, 2055151.

2.2.8. Complexes of 4-((Ethoxycarbonyl)biphenyl-4-yl)-2,2':6',2''-terpyridine, Ebptpy

(25) **[Ni(ebptpy)₂](ClO₄)₂·3DMF**: Ni(ClO₄)₂·6H₂O (8.0 mg, 0.022 mmol) in DMF (5 mL) was added to **ebptpy** (20 mg, 0.044 mmol) in DMF (10 mL). The resulting solution was heated for 2 h at 100 °C before the solvent was removed under reduced pressure. The yellow residue was washed with methanol and chloroform and then dried at ambient temperature (yield: 21 mg, 69%). Anal. calc. for C₆₉H₆₇Cl₂N₉NiO₁₅: C, 59.54; H, 4.85; N, 9.06. Found: C, 59.60; H, 4.53; N, 9.21%. The vapour diffusion of methanol into a DMF solution of the complex produced yellow, rod-like crystals suitable for X-ray diffraction studies. CCDC number, 2055152.

(26) **[Cu(ebptpy)₂](ClO₄)₂·CH₃CN**: Cu(ClO₄)₂·6H₂O (8.1 mg, 0.022 mmol) in DMF (5 mL) was added to **ebptpy** (20 mg, 0.044 mmol) in DMF (10 mL). The resulting solution was heated for 2 h at 100 °C before the solvent was removed under reduced pressure. The green residue was washed with methanol and chloroform, and dried at ambient temperature (yield: 0.018 g, 67%). Anal. calc. for C₆₂H₄₉Cl₂N₇CuO₁₂: C, 61.11; H, 4.05; N, 8.05. Found: C, 60.99; H, 4.02; N, 8.10%. The vapour diffusion of diethyl ether into an acetonitrile solution of the complex provided green, rod-like crystals suitable for X-ray diffraction studies. CCDC number, 2055153.

2.2.9. Zinc(II) Complex of 4-((Ethoxycarbonyl)terphenyl-4-yl)-2,2':6',2''-terpyridine, etptpy

(27) **[Zn(etptpy)₂](ClO₄)₂·2DMF·H₂O**: Zn(ClO₄)₂·6H₂O (7.0 mg, 0.016 mmol) in DMF (5 mL) was added to **etptpy** (20 mg, 0.037 mmol) in DMF (10 mL). After stirring the

resulting solution for 2 h at 100 °C, the solvent was removed under reduced pressure. The white residue was washed with methanol and chloroform and then dried at ambient temperature (yield: 19 mg, 84%). Anal. calc. for $C_{75}H_{61}Cl_2N_7O_{13}Zn$: C, 64.13; H, 4.38; N, 6.98. Found: C, 64.08; H, 4.52; N, 6.70%. 1H -NMR (300 MHz) in DMSO- d_6 : δ 9.50 (s, 4H), 9.23 (d, $J = 7.5$ Hz, 4H), 8.62 (d, $J = 7.5$ Hz, 4H), 8.33 (t, $J = 6.8$ Hz, 4H), 8.21 (d, $J = 7.7$ Hz, 4H), 8.13 (t, $J = 8.0$ Hz, 8H), 7.99 (m, 12H), 7.55 (t, $J = 5.5$ Hz, 4H), 4.41 (q, $J = 6.7$ Hz, 4H, $-CH_2-$), 1.40 (t, $J = 7.2$ Hz, 6H, $-CH_3$). The vapour diffusion of methanol into a DMF solution of the complex produced pale-yellow, rod-like crystals suitable for X-ray diffraction studies. CCDC number, 2055154.

2.2.10. Complexes of 4'-(Benzyloxy)-2,2':6',2''-terpyridine, **bzOtpy**

(28) [Fe(bzOtpy) $_2$](ClO $_4$) $_2$: A mixture of Fe(ClO $_4$) $_2$ ·6H $_2$ O (12 mg, 0.033 mmol) and **bzOtpy** (30 mg, 0.088 mmol) in CH $_2$ Cl $_2$ /CH $_3$ OH (20 mL, 1:1, v/v) was heated under reflux for 2 h. Upon cooling, the solvent was evaporated off under reduced pressure. The purple residue was washed with methanol and dichloromethane and dried at ambient temperature (yield: 30 mg, 97%). Anal. calc. for $C_{44}H_{34}Cl_2N_6FeO_{10}$: C, 56.61; H, 3.67; N, 9.00. Found: C, 56.48; H, 3.89; N, 9.11%. 1H -NMR (300 MHz) in CD $_3$ CN: δ 8.60 (s, 4H), 8.47 (d, $J = 7.8$ Hz, 4H), 7.92 (t, $J = 7.7$ Hz, 4H), 7.77 (d, $J = 7.5$ Hz, 4H), 7.64 (m, 6H), 7.20 (d, $J = 5.4$ Hz, 4H), 7.13 (t, $J = 6.4$ Hz, 4H), 5.72 (s, 4H, $-CH_2-$). The slow evaporation of an acetonitrile solution of the complex at ambient temperature produced purple crystals suitable for X-ray diffraction studies. CCDC number, 2055155.

(29) [Ni(bzOtpy) $_2$](ClO $_4$) $_2$: Ni(ClO $_4$) $_2$ ·6H $_2$ O (17 mg, 0.047 mmol) and **bzOtpy** (30 mg, 0.088 mmol) were dissolved in CH $_2$ Cl $_2$ /CH $_3$ OH (20 mL, 1:1, v/v) and heated under reflux for 2 h. Upon cooling, the solvent was evaporated off under reduced pressure. The yellow residue was washed with methanol and dichloromethane and then dried at ambient temperature (yield: 36 mg, 82%). Anal. calc. for $C_{44}H_{34}Cl_2N_6NiO_{10}$: C, 56.44; H, 3.66; N, 8.98. Found: C, 56.70; H, 3.74; N, 9.08%. The slow evaporation of an acetonitrile solution of the complex at ambient temperature produced purple crystals suitable for X-ray diffraction studies. CCDC number, 2055156.

2.2.11. 4'-(3,4,5-Trimethoxy-phenyl)-2,2':6',2''-terpyridine, **tmptpy**, and its Zn(II) Complex

(30) Tmptpy [34] in its diprotonated form as the perchlorate salt, hemi-tetrahydrofuran solvate, [H $_2$ tmptpy](ClO $_4$) $_2$ ·0.5THF: **tmptpy** (100 mg) was dissolved in THF (30 mL), and 1 mL of 1 M HClO $_4$ was added with stirring over 30 min, after which the solution was allowed to slowly evaporate under ambient temperature to produce colourless crystals suitable for structure determination. Anal. calc. for $C_{52}H_{54}Cl_4N_6O_{23}$: C, 49.07; H, 4.28; N, 6.60; Found: C, 48.54; H, 4.31; N, 6.48%. CCDC number, 2055157.

(31) [Zn(tmptpy) $_2$](ClO $_4$) $_2$ ·CH $_3$ CN: Zn(ClO $_4$) $_2$ ·6H $_2$ O (7.0 mg, 0.016 mmol) in DMF (5 mL) was added to **tmptpy** (20 mg, 0.037 mmol) in DMF (10 mL). The solvent was removed under reduced pressure after stirring the solution for 2 h at 100 °C. The white residue was washed with methanol and chloroform and then dried at ambient temperature (yield: 19 mg, quantitative). Anal. calc. for $C_{50}H_{45}Cl_2N_7O_{14}Zn$: C, 54.39; H, 4.11; N, 8.88. Found: C, 54.44; H, 4.08; N, 8.96%. 1H -NMR (300 MHz) in CD $_3$ CN: δ 9.00 (s, 4H), 8.82 (dt, $J = 8.1, 0.8$ Hz, 4H), 8.23 (td, $J = 7.8, 1.7$ Hz, 4H), 7.87 (dq, $J = 5.1, 0.6$ Hz, 4H), 7.46 (dd, $J = 5.1, 1.0$ Hz, 2H), 7.44 (s, 4H), 7.43 (dd, $J = 5.1, 1.0$ Hz, 2H), 4.10 (s, 12H, $-CH_3$), 3.92 (s, 6H, $-CH_3$). The vapour diffusion of methanol into a DMF solution of the complex produced pale-yellow, rod-like crystals suitable for X-ray diffraction studies. CCDC number, 2055158.

2.2.12. Complexes of

2-(4-(2-(3,4,5-Trimethoxyphenyl)Ethynyl)-6-(pyridin-2-yl)pyridin-2-yl)pyridine, **tmpatpy**

(32) [Ni(tmpatpy)₂](ClO₄)₂·CH₃CN·H₂O: Ni(ClO₄)₂·6H₂O (9.0 mg, 0.025 mmol) in acetonitrile (5 mL) was added to **tmpatpy** (20 mg, 0.047 mmol) in CH₃CN/CHCl₃ (10 mL, 1:1, *v/v*). After stirring the resulting solution for 1 h at 60 °C, the solvent was removed under reduced pressure. The yellow residue was washed with methanol and chloroform and then dried at ambient temperature (yield: 21 mg, 57%). Anal. calc. for C₁₀₆H₈₉Cl₄N₁₃O₂₉Ni₂: C, 56.13; H, 3.96; N, 8.03. Found: C, 56.22; H, 3.98; N, 8.11%. The slow evaporation of an acetonitrile solution of the complex at ambient temperature provided yellow, rod-like crystals suitable for X-ray diffraction studies. CCDC number, 2055159.

(33) [Zn(tmpatpy)₂](ClO₄)₂·CH₃CN·3H₂O: Zn(ClO₄)₂·6H₂O (9.0 mg, 0.024 mmol) in acetonitrile (5 mL) was added to **tmpatpy** (20 mg, 0.047 mmol) in CH₃CN/CHCl₃ (10 mL, 1:1, *v/v*). After stirring the resulting solution for 1 h at 60 °C, the solvent was removed under reduced pressure, and the bright yellow residue was washed with methanol and chloroform, and then dried at ambient temperature (yield: 22 mg, 76%). Anal. calc. for C₅₄H₅₁Cl₂N₇O₁₇Zn: C, 53.77; H, 4.26; N, 8.13. Found: C, 53.57; H, 4.20; N, 8.18%. ¹H-NMR (300 MHz) in CD₃CN: δ 8.86 (s, 4H), 8.60 (dt, *J* = 8.1, 0.8 Hz, 4H), 8.22 (td, *J* = 7.7, 1.6 Hz, 4H), 7.86 (dq, *J* = 5.1, 0.8 Hz, 4H), 7.46 (dd, *J* = 5.1, 1.0 Hz, 2H), 7.43 (dd, *J* = 5.1, 0.9 Hz, 2H), 7.10 (s, 4H), 3.95 (s, 12H, -CH₃), 3.85 (s, 6H, -CH₃). The slow evaporation of an acetonitrile solution of the complex at ambient temperature provided pale yellow, rod-like crystals suitable for X-ray diffraction studies. CCDC number, 2055160.

(34) [Ru(tmpatpy)₂](PF₆)₂·1.5DMF: A mixture of **tmpatpy** (50 mg, 0.12 mmol) and RuCl₃·*x*H₂O (25 mg) in ethanol (30 mL) was heated at 70 °C for 4 h to produce a turbid, reddish-purple solution. This was cooled to ambience to produce a precipitate of a brown powder, washed on the filter with ethanol, which was assumed to be [Ru(**tmpatpy**)Cl₃]. [Ru(**tmpatpy**)Cl₃] (40 mg, 0.063 mmol), **tmpatpy** (30 mg, 0.071 mmol) and *N*-ethylmorpholine (five drops) were dissolved in CH₃OH/CHCl₃ (40 mL, 3:1, *v/v*) and heated at 70 °C for 2 h. The resultant deep red solution was filtered through Celite to remove some insoluble purple material, and the solvent was evaporated under reduced pressure. The dark red residue was dissolved in a minimum volume of acetonitrile and loaded on a short silica column, and the column was eluted with acetonitrile/saturated aqueous KNO₃/water (7:1:0.5, *v/v*). The major red component was collected, methanolic NH₄PF₆ was added, and 1 h was allowed for the precipitation of a red powder, which was then collected, washed on the filter with methanol and dried under vacuum (yield: 35 mg, 41%). Anal. calc. for C₁₁₃H₁₀₅F₂₄N₁₅O₁₅P₄Ru₂: C, 50.36; H, 3.93; N, 7.80. Found: C, 50.41; H, 3.80; N, 7.78%. ¹H-NMR (300 MHz) in CD₃CN: δ 8.88 (s, 4H), 8.54 (dq, *J* = 8.2, 0.8 Hz, 4H), 8.01 (td, *J* = 7.7, 1.5 Hz, 4H), 7.45 (dq, *J* = 5.5, 0.6 Hz, 4H), 7.24 (dd, *J* = 5.6, 1.3 Hz, 2H), 7.22 (dd, *J* = 5.6, 1.3 Hz, 2H), 7.09 (s, 4H), 3.96 (s, 12H, -CH₃), 3.85 (s, 6H, -CH₃). The slow evaporation of an acetonitrile solution of the complex provided red crystals suitable for X-ray structure determination. CCDC number, 2055161.

3. Crystallography

Diffraction data for crystals of complexes **1–3**, **7–18**, **20**, **21**, **23–28** and **30–33** were obtained at 100(2) K using an ADSC Quantum 210 detector at 2D SMC with a silicon (111) double crystal monochromator (DCM) for various synchrotron wavelengths between 0.62988 and 0.75000 Å at the Pohang Accelerator Laboratory, Pohang, South Korea. The ADSC Q210 ADX program [51] was used for data collection (detector distance, 63 mm; omega scan; Δω = 1°; exposure time, 1 s per frame), and HKL3000sm (Ver. 703r) [52] was used for cell refinement, reduction and absorption correction. The structures were solved by direct methods and refined by full-matrix least-squares fitting on *F*² using SHELXL-2014 [53]. All the non-hydrogen atoms were refined with anisotropic displacement parameters. The carbon-bound hydrogen atoms were introduced at

calculated positions, and all the hydrogen atoms were treated as riding atoms with an isotropic displacement parameter equal to 1.2 times that of the parent atom.

Diffraction data for complexes **4–6**, **19**, **22**, **29** and **34** were obtained on a RIGAKU Saturn CCD diffractometer with a confocal mirror, using graphite-monochromated Mo K_{α} radiation ($\lambda = 0.71073 \text{ \AA}$) or, for **19** only, Cu K_{α} radiation ($\lambda = 1.54187 \text{ \AA}$). The structures were solved by direct methods and refined on F^2 by full-matrix least-squares treatment [53].

For complexes **7**, **9**, **13**, **14**, **18**, **20**, **28**, **29**, **32** and **34**, the SQUEEZE option of PLATON [54] was used to take into account the contribution of disordered solvents during refinement. The results (the size of the voids, number of electrons present in the voids and possible solvent molecules present) are summarized in Table S1.

Full details of all the structure determinations have been deposited as cifs in the Cambridge Crystallographic Data Collection under CCDC deposition numbers 2055133-2055135, 2055137-2055142, 2055148-2055161 and 2055219-2055228. Note that for structures **7** and **9**, the solutions were unsatisfactory in that the residual (R_I factor) exceeded 0.10, but they have been included for comparative purposes.

The nature of the atoms involved in the interactions exceeding dispersion was established using CrystalExplorer [30], and their specific identities (atom numbers and locations) were established using CrystalMaker [55], which was then used to prepare figures with the interactions shown as dashed lines. In the case of the complexes for which SQUEEZE was applied during the structure refinement (see above), the Hirshfeld surfaces calculated with CrystalExplorer may lack indications of some interactions since not all the solvent molecules present were included in the calculation.

4. Results and Discussion

Most of the ligands used in the present work are well-known species for which the coordination chemistry is well-established. We have described in detail, elsewhere [33], the syntheses of three new ligands (**bzOtpy**, **etptpy** and **pfatpy**) and, here, that of **papatpy** (Figure 1), closely based on methods established for related compounds, as were the syntheses of their metal-ion complexes, so a detailed discussion of these aspects of the present work is not warranted. With the exception of the kinetically inert Ru(III) ions, the metal ions used herein are all labile species, so the synthesis of their complexes is trivial. The crystallisation of the complexes in a form suitable for X-ray diffraction measurements was not necessarily trivial and generally involved the exploration of several methods, although only in the case of complexes of **pfatpy** were real difficulties encountered, these being such that only a single complex of this ligand was structurally characterised. In regard to the coordination spheres of the metal ions and the stacking tendency of the cations in the 33 compounds structurally characterised, nothing setting them apart from their extensive context is apparent, and our focus was on just the solid-state interactions discernible from analysis of the Hirshfeld surfaces.

As a background to the analysis of the crystal structures of complexes of 4'-substituted 2,2':6',2''-terpyridine, it is useful to consider the structures of free ligands that are available, although these are relatively limited in number, and this we have done in a separate work [37]. All free terpyridines show non-chelating, bis-transoid arrays of the three N-donor atoms, except in the case of the 4'-hydroxy derivative, which exists as a 1:1 mixture of the hydroxypyridine and pyridone tautomers in the solid state [56–58], where the pyridone tautomer adopts a bis-cisoid array, while the hydroxypyridine form has a bis-transoid form. Significantly, although the stacking of the terpyridine units is a common feature of free ligand structures, this appears in most instances other than those where large, polar substituents are present, to be associated simply by dispersion interactions between terpyridine units, and only the pyridone tautomer of 4'-hydroxy-2,2':6',2''-terpyridine is clearly involved in additional, specific C...C interactions between facing aromatic planes, with interactions of the peripheral H-atoms being the dominant form of interactions, exceeding dispersion in all cases.

While much of the interest in 2,2':6',2''-terpyridine chemistry has been focused on metal-ion complexes in low oxidation states [1–7], complexes of high-oxidation-state metal ions are also known, with vanadium(V) [59] and uranium(VI) (as the uranyl ion, UO_2^{2+}) [60–63] providing examples of extremes. In that the formation of a coordinate bond is formally a process where the metal ion gains electrons and the ligand loses them, such extreme cases might be expected to be associated with charge redistribution favouring the appreciable interaction of the bound ligand with nucleophiles, akin to the addition to an imine bond. In the case of crystalline $[\text{VO}_2(\text{btpy})]\text{ClO}_4$, **1**, the Hirshfeld surfaces of the two inequivalent cations provide evidence for exactly this, with the most marked region of interaction exceeding dispersion, that being due to the contact of vanadyl-O (O1) with one of the carbon atoms (C10) adjacent to the central N-atom of the ligand (Figure 2a). Reciprocal, remarkably short contacts ($\text{O1}\cdots\text{C10}^i = \text{O1}\cdots\text{C10}$, 2.81(1) Å; $i = 1 - x, 1 - y, 2 - z$) of this type result in the presence of pairs of the two inequivalent cations, where the slightly bowed terpyridine units lie close to parallel, with a separation of ~ 3.5 Å, and where there are only barely perceptible indications of other interactions beyond the dispersion of the C and H atoms of ligand units lying both close to parallel and nearly perpendicular to the ligand of the cation considered (Figure S1). Multiple interactions involving peripheral aromatic H-atoms and vanadyl- or perchlorate-O atoms serve to link the whole structure together, but none involve unusually short contacts, and as is seen in the examples discussed later, they appear to be a common feature of structures regardless of the metal ion present. However, as some interactions involve the 4'-biphenyl substituent on the terpyridine unit, it is unsurprising that there are significant differences in the structure of the “parent” species $[\text{VO}_2(\text{tpy})]\text{ClO}_4$ [59] when compared to that of **1** (Figure 2b). Here, the most obvious interaction beyond the dispersion of a given cation again involves the contact of a O-atom with a C adjacent to a N, but the O-atom is from perchlorate, and two adjacent C atoms, one from the central and one from an outer pyridine unit ($\text{O4}\cdots\text{C6}$, 3.09(1) Å; $\text{O4}\cdots\text{C5}$, 3.162(8) Å), are involved. Vanadyl-O...C contacts are still apparent and are associated with the maintenance of a stacked arrangement of (equivalent-) cation pairs but involve C-atoms separated by another from N ($\text{O1}\cdots\text{C4}'$, 3.162(8) Å; $i' = 1 - x, 1 - y, 2 - z$). Note that while in **1**, the nearer phenyl ring of the biphenyl substituent is close to coplanar with the terpyridine unit, indicating, possibly, a degree of delocalisation as an influence upon the electronic properties of the whole, this is also seen in some M(II) complexes of the ligand [43] and appears to be a consequence of CH interactions with counteranions.

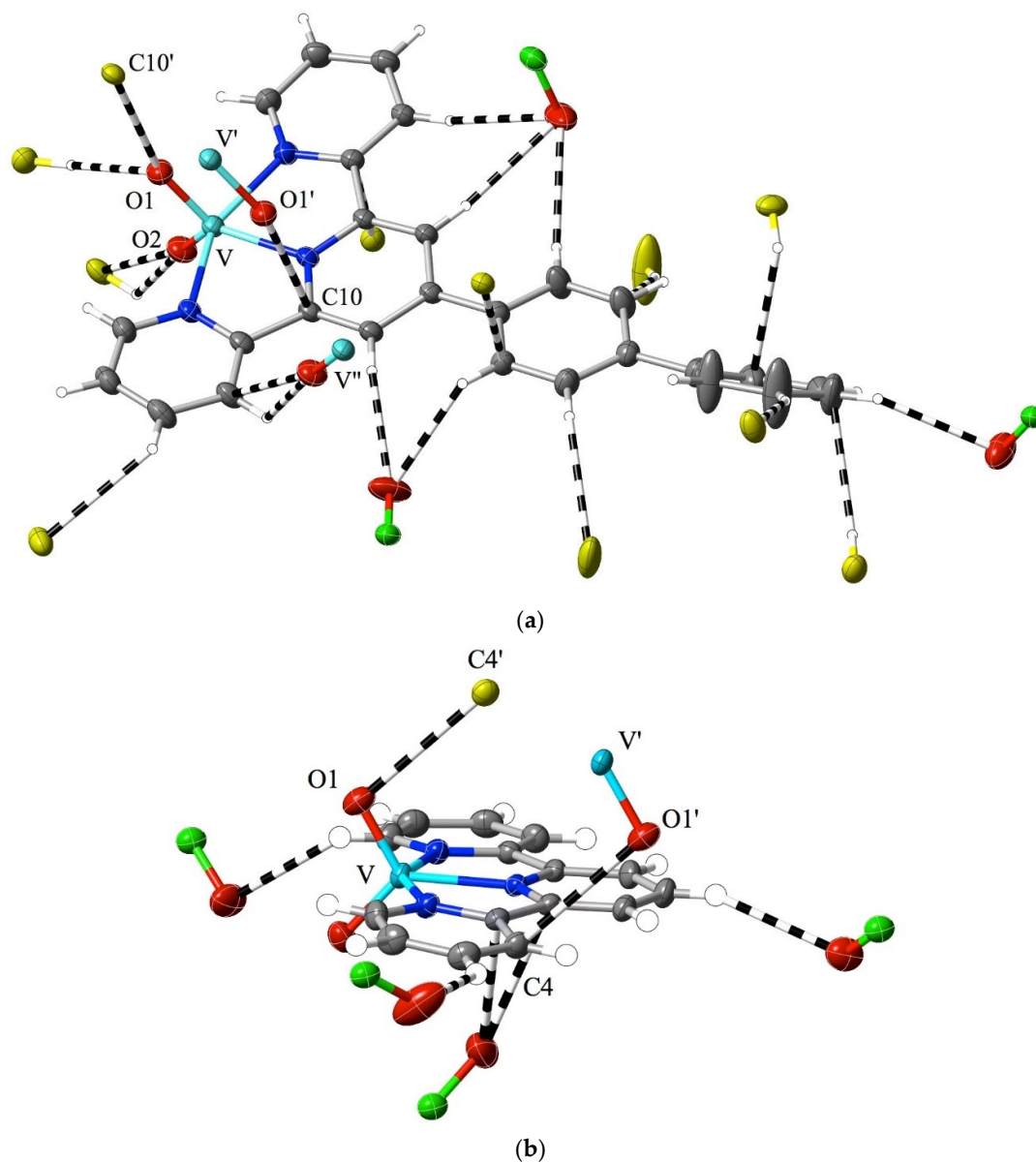


Figure 2. Interactions beyond dispersion, shown as dashed lines, of the cations present in (a) $[\text{VO}_2(\text{bptpy})]\text{ClO}_4$, **1** and (b) $[\text{VO}_2(\text{tpy})]\text{ClO}_4$ [44]. O atoms are identified by showing the atoms to which they are attached. Colour coding: C = grey, N = dark blue, O = red, Cl = green, and V = light blue, except for carbon atoms from adjacent cations, which are shown in yellow. H-atoms are shown as small, colourless spheres of arbitrary 0.2 Å radius.

In known structures of uranyl-ion complexes of 2,2':6',2''-terpyridine [60–63] (and, in some cases [60,61], of 4'-chloro-2,2':6',2''-terpyridine), the close contact of at least one O-atom with one or two C-atoms bound to the N of another complex forming a stacked array is common but not universal. In $[\text{UO}_2(\text{tpy})(\text{tdc})_2]$ (**tdc** = thiophene-1,4-dicarboxylate) and its chloroterpyridine analogue [45], there are such contacts with $\text{C6}\cdots\text{O2}'(\text{uranyl})$ 3.039(5) Å and $\text{C6}\cdots\text{O4}'(\text{carboxylate})$ 2.947(8) Å, respectively, although much more obvious in the former are reciprocal uranyl-O2...N2' contacts of 2.783(4) Å (Figure S2a). In $[(\text{UO}_2)_2(\text{OH})(\text{tpy})(\text{dcb})_3]$ (**dcb** = 3,5-dichlorobenzoate) and its chloroterpyridine analogue [61], there are contacts with $\text{C15}\cdots\text{O2}'(\text{uranyl})$ 3.014(7) Å and $\text{C15}\cdots\text{O2}'(\text{uranyl})$ 2.915(6) Å, respectively, while in $[(\text{UO}_2)_2(\text{OH})_2(\text{tpy})_2](\text{ClO}_4)_2$ [62], where there are two inequivalent dimers within the structure, the C–O contacts $\text{C5}\cdots\text{O8}'(\text{uranyl})$

2.949(6) Å, C6··O8'(uranyl) 2.959(7) Å and C41··O2'(uranyl) 2.953(6) Å are apparent (Figure S2b). In [UO₂(tpy)(bpdc)] (bpdc = 2,2'-bipyridine-3,3'-dicarboxylate) [63], there is a similarly short contact of C5··O1'(uranyl) 2.937(3) Å, but in the four complexes [UO₂(tpy)(tph)] and [UO₂(tpy)(npdc)] (tph = terephthalate {benzene-1,4-dicarboxylate}; npdc = naphthalene-1,4-dicarboxylate) and their chloroterpyridine analogues, such interactions are not evident. Here, extended stacking arrays of the aromatic units appear to block the access of other species to C-atoms bound to N in the ligand. This is a timely reminder that any weak interactions beyond dispersion evident in a Hirshfeld surface representation are exactly that, weak, and that the balance between any number of such interactions may be extremely sensitive to compositional differences.

If a positive charge on a bound metal does produce charge depletion on the ligand in the region of the donor atoms, then any effect should diminish with a decreasing charge, and the smallest positive charge is that carried by the proton, H⁺. The diprotonation of a terpyridine is required to produce the di-cisoid configuration found in metal-ion complexes such as **1**, and the structure of compound **30**, [H₂tmptpy](ClO₄)₂·0.5THF, adds to several known for such species. (A summary of relevant literature is given in [33].) Here, as is broadly true [33], there is no evidence on the Hirshfeld surface, except for an indication that the interaction of one perchlorate-O (O17) may be better considered as involving the C25–H25 bond rather than H25 alone, for interactions of nucleophiles with C-atoms attached to any of the N-donor atoms, and this is consistent with what is seen in complex **1** and several other species discussed above, being evidence for the significant polarising effects of highly charged cations. Peripheral CH··O interactions of aromatic CH with perchlorate-O, however, are numerous, and the cations lie in infinite stacks largely involving dispersion interactions only, except for barely discernible C··C interactions between alternate pairs of the two inequivalent cations of the structure, with C11··C44ⁱ 3.31(4) Å and C18··C29ⁱ 3.34(4) Å (*i* = *x* + 0.5, *y* + 0.5, *z*) (Figure 3). While the atoms C11 and C29 are adjacent to N in the terpyridine unit, C18 and C44 are C-atoms of the substituent to which methoxy groups are attached, showing that purely dispersive stacking of the terpyridine units as seen in unfunctionalised ligand salts such as [H₂tpy]Cl₂·H₂O [64] can be disrupted by substituents.

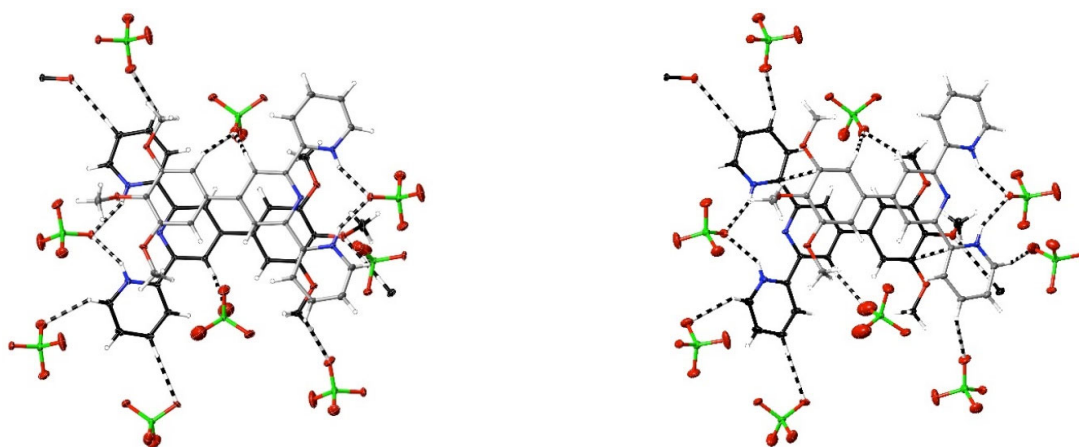
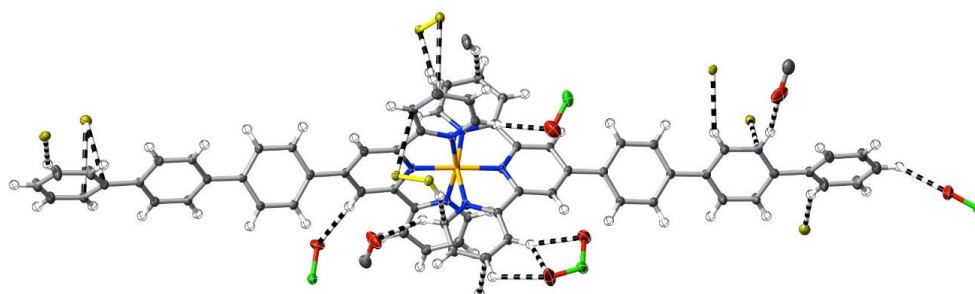


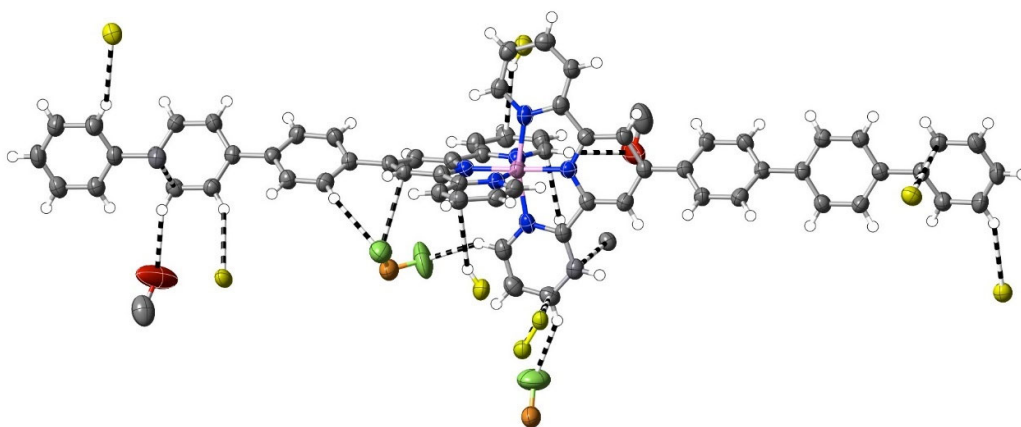
Figure 3. Views perpendicular (left) and at 30° (right) to the mean plane of one of the stacked pairs of inequivalent cations found in the structure of [H₂tmptpy](ClO₄)₂·0.5THF, **30**, showing (dashed lines) the interactions exceeding dispersion of the cations. Carbon atoms of one cation are shown in black; of the other, in grey. C–C interactions are visible in the 30° view.

The vast majority of the structural studies of complexes of 2,2':6',2''-terpyridine and its derivatives concern metal(II) and metal(III) species, and the present work largely complements such investigations, which range, for Co(II), for example, from early determinations on a single compound for which H-atom coordinates are not available, e.g., [65], to those of several complexes of various derivatives with full coordinates, e.g., [66], such

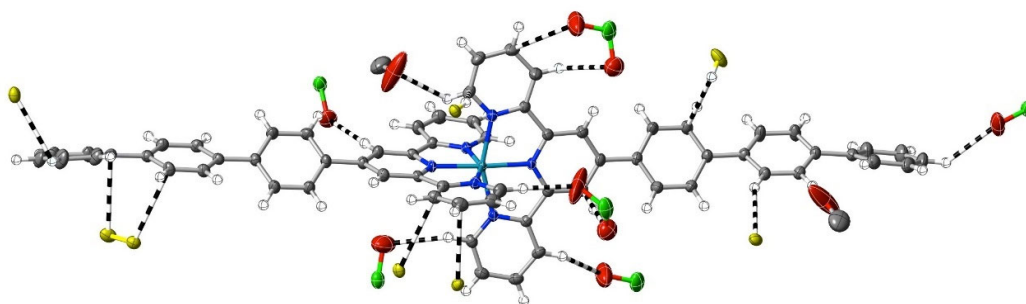
variations reflecting, in part, major advances in the ease of the synthesis of the ligands [1–7] and in crystallographic equipment. The complexes **2–6** of the **tptpy** ligand add Fe(II), Ni(II) and Ru(II) to the series, with Co(II), Cu(II), Zn(II) and Cd(II) studied earlier [34,37], and form part of a rather large family of structurally characterised complexes of 4' derivatives of 2,2':6',2''-terpyridine, where the substituent is an apolar aromatic unit. An obvious question to ask in relation to the nine structures of 4'-terphenyl-2,2':6',2''-terpyridine we studied is whether or not the changes in the electron configurations of the exclusively M(II) cations involved have an effect detectable in the form of the Hirshfeld surfaces of the complexes in the solid state. The answer is that none is clearly evident. A feature of all the structures is that the terphenyl tail is significantly twisted, both within its chain and relative to the terpyridine unit, indicating that there is no extended delocalisation within the whole ligand and, thus, that the addition of the terphenyl tail does not produce a larger, planar aromatic unit that might engage in stronger stacking interactions than in simple 2,2':6',2''-terpyridine complexes. It is certainly possible to discern aromatic and aza-aromatic entities that form arrays of "face-to-face" and "edge-to-face" types, and these are associated with various C–C and CH–C (CH– π) interactions that exceed dispersion and are thus evident on the Hirshfeld surfaces. In the totality of the interactions exceeding dispersion (Figure 4), there is no evidence for nucleophile addition to C-atoms adjacent to N, so it can be said at this point that M(II) cations seem to be distinguishable from M(V) and M(VI) cations in this respect. Interactions of the cations with the counteranions and lattice solvents occur along with aromatic–aromatic interactions, and even in only the eight cases considered, there are variations in both the counteranions and lattice solvents as well as in the space groups, so it is unsurprising that there are differences in the exact patterns of interactions across the eight, but in every one, there are C–C and CH–C interactions beyond dispersion with both the tpy head groups and at least one of the phenyl groups of the tails. A comparison of the mixed-ligand complexes **5** and **6** shows that aromatic–aromatic interactions beyond dispersion are little affected by the difference in anion, indicating that aromatic–aromatic interactions in general, including dispersion, may be the dominant factor influencing the array of cations in the crystal. Analysis (Figure S3) of the structures reported [43] for a family of complexes of the ligand 4'-biphenyl-2,2':6',2''-terpyridine (**bptpy**) confirms the observation that for a similar range of M(II) species (M = Co, Ni, Cu, Zn, Cd and Ru), none provides evidence of significant weak interaction with C-atoms bound to N, though perhaps because of the differences in temperature for the present and these earlier determinations, the C–C and CH–C interactions beyond dispersion between aromatic/aza-aromatic units are generally less numerous for the **bptpy** derivatives. The known structures for the Co(II) [37] and Zn(II) [35] complexes of the very long-tailed 4'-quaterphenyl-2,2':6',2''-terpyridine (**qptpy**) ligand provide no exceptions to the observation of a lack of any enhanced electrophilicity of C-atoms bound to coordinated N, just like the very numerous structures of complexes of 2,2':6',2''-terpyridine itself and its 4'-phenyl and -4-methylphenyl (tolyl) derivatives, where, however, there are examples of M(III) complexes where the generalisation appears to be valid (M = Co, Rh) [67,68] and at least one (M = Cr) [69] where it is not. It is, of course, well-known [70] that the synthesis of functionalised aza-aromatic ligands can be based on nucleophilic attack on precisely the C-atoms adjacent to N.



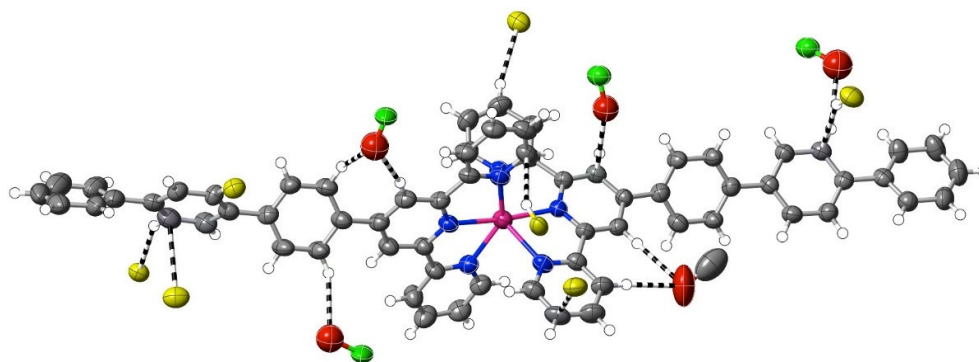
(a) $[\text{Fe}(\text{tptpy})_2](\text{ClO}_4)_2 \cdot \text{CH}_3\text{OH}$ (Fe = orange), **2**.



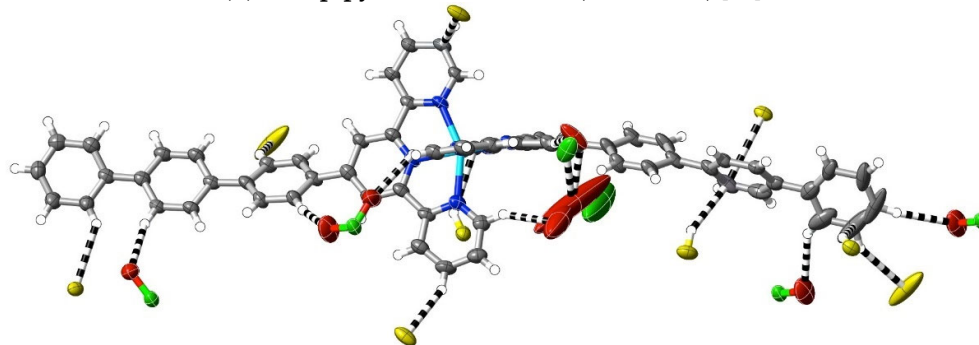
(b) [Co(tppty)₂](BF₄)₂·CH₃OH (Co = pink; B = brown) [37].



(c) [Ni(tppty)₂](ClO₄)₂·CH₃OH (Ni = turquoise), 3.



(d) [Cu(tppty)₂](ClO₄)₂·CH₃OH (Cu = violet) [34].



(e) [Zn(tppty)₂](ClO₄)₂·DMF (Zn = sky blue) [34].

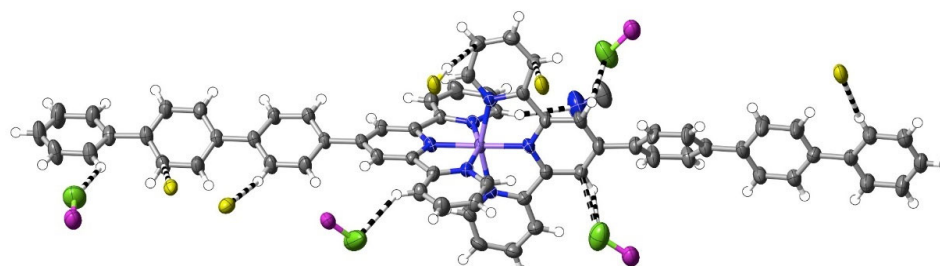
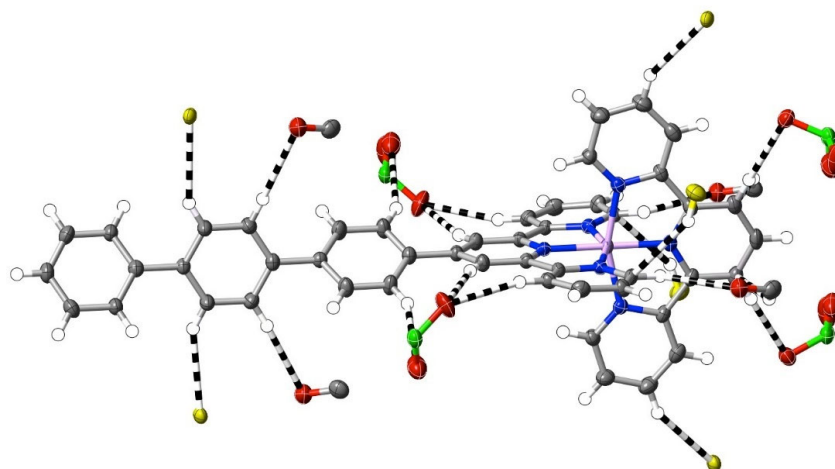
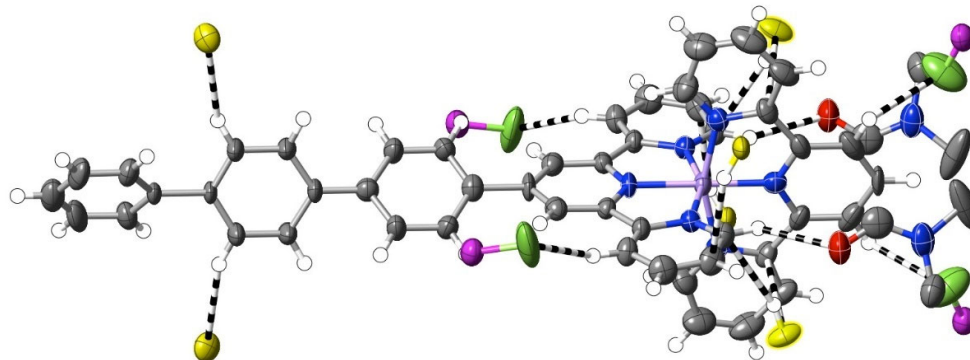
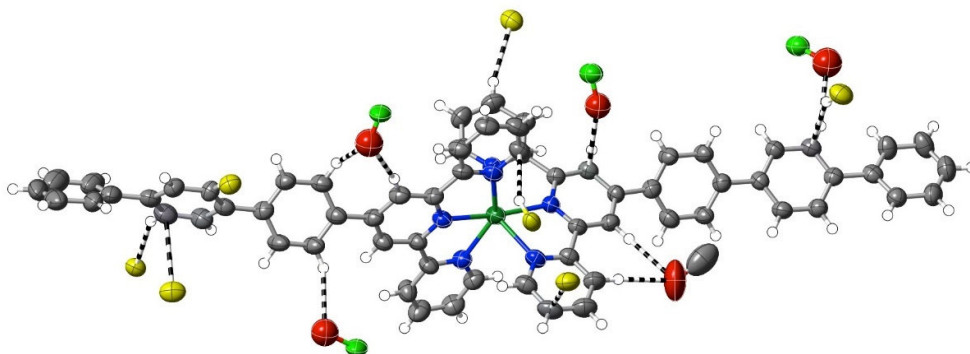
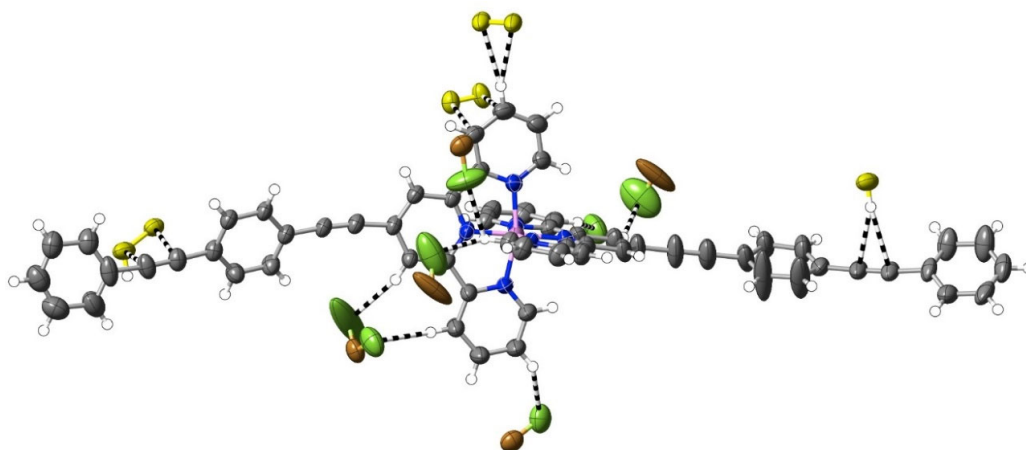
(f) $[\text{Ru}(\text{tptpy})_2](\text{PF}_6)_2$ (Ru = mauve), 4.(g) $[\text{Ru}(\text{tptpy})(\text{tpy})](\text{ClO}_4)_2 \cdot 2\text{DMF}$ (Ru = mauve), 5.(h) $[\text{Ru}(\text{tptpy})(\text{tpy})](\text{PF}_6)_2 \cdot 2\text{DMF}$ (Ru = mauve), 6. (Non-disordered cation.)(i) $[\text{Cd}(\text{tptpy})_2](\text{ClO}_4)_2 \cdot \text{DMF} \cdot 0.5\text{H}_2\text{O}$ (Cd = dark green) [34].

Figure 4. Interactions exceeding dispersion (dashed lines) of cations complexed by 4'-terphenyl-2,2':6',2''-terpyridine. As in Figure 1, C-atoms of ligands not directly bound to the one metal ion involved are shown in yellow. Different O-atoms involved are identified by their attached atoms (e.g., Cl for perchlorate-O).

A different means of extending an apolar 4' tail on 2,2':6',2''-terpyridine is seen in complexes 7–16, where ethynyl units serve to link phenyl rings. Although initially envisaged as sites of polarisable electron density that might give rise to significant interactions beyond dispersion, the ethynyl units have, at most, a limited role of this type in any of the 10 complexes characterised (as well as in the complexes 32–34 of the further-functionalised phenylethynyl ligands—see below). Thus, as shown in Figure 5, in the Co(III) complex 9 of **papatpy**, one outer ethynyl group is involved in C··C interactions, and the other, in one CH··C interaction (with both C-atoms), while in the Ni(II) complex 10, one inner unit is involved in a C··HC interaction (again with both C-atoms to one H), but in the Cu(II) complex 11 and the Zn(II) complex 12, there are no interactions beyond dispersion with any ethynyl unit, as is the case for the Zn(II) complex 7 of **patpy**. In the Ru(II) complex 13, there are C··C interactions with one outer ethynyl unit, but in the mixed-ligand **papatpy-tpy** Ru(II) complex 14, there are no interactions, as is the case in the 1:2 and 1:1 complexes 15 and 16, respectively, of **papatpy** with Cd(II) and also in the complex 17 of **pfpatpy** with Fe(II). All the structures 7–16 were determined at 100(2) K, so temperature, for which there is some evidence of influence in the determination of the visibility of weak interactions (see ahead), cannot be considered as a factor determining these observed variations in ethynyl group interactions. What, of course, should be noted is that the multiple prominent interactions apparent in all the cases are those with anion atoms (O, F or Cl), and while these tend to be concentrated close to the formal positive site of the metal ion, they also occur with the extremities of the complexes, again consistent with the notion that both dispersive interactions and those that exceed them are involved in a delicate balance that may vary with changes such as that of the anion or uncoordinated solvent but also minor factors such as bond length changes and stereochemical preferences (for example, where the Jahn–Teller effect renders the coordination sphere of Cu(II) somewhat more irregular than that for other metal ions). Thus, the pattern of interactions exceeding dispersion is different in every complex and shows no obvious correlation with electron configurations, though the Ni(II) complex 10 does provide an example where there are (perchlorate)O··C interactions involving C-atoms bound to N-donors. This is an unusual example where a single O-atom is in interaction with four C-atoms, two of which are directly bound to N and two of which are not, so each individual interaction may be reinforced by the other three. A clearer situation of nucleophile interaction with C bound to an N-donor, however, is found in complex 17 (Figure 6), where an aryl-F atom bridges C-atoms adjacent to N on separate ligand units. In fact, the F-atom substituents of the **pfpatpy** ligand are also involved in multiple interactions beyond dispersion that link different cations together, providing the first example in the present study of a marked effect of ligand substituents on secondary interactions.



(a) $[\text{Co}(\text{papatpy})_2](\text{BF}_4)_3 \cdot 2\text{CH}_3\text{CN}$, 9.

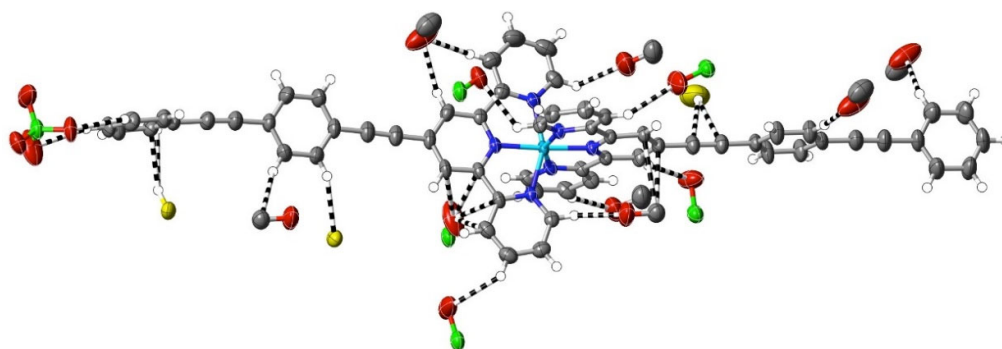
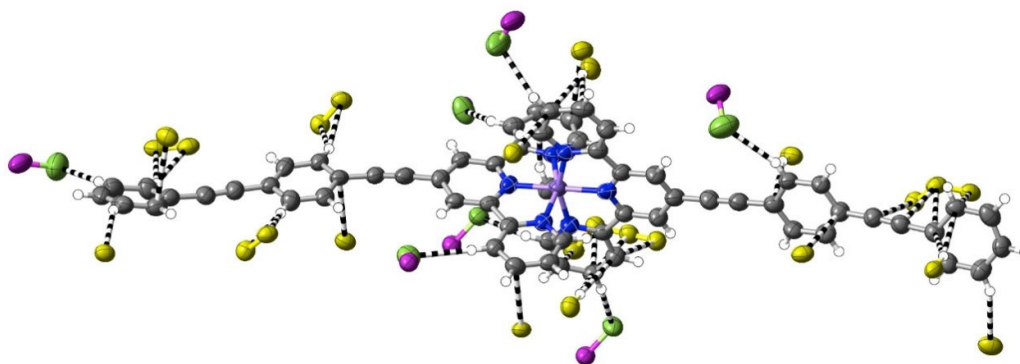
(b) $[\text{Ni}(\text{papatpy})_2](\text{ClO}_4)_2 \cdot 3\text{DMF}$, 10.(c) $[\text{Ru}(\text{papatpy})_2](\text{PF}_6)_2$, 13.

Figure 5. Interactions beyond dispersion involving the ethynyl subunits in complexes of phenylethynyl derivatives of 2,2':6',2''-terpyridine. Colour coding as in Figure 1.

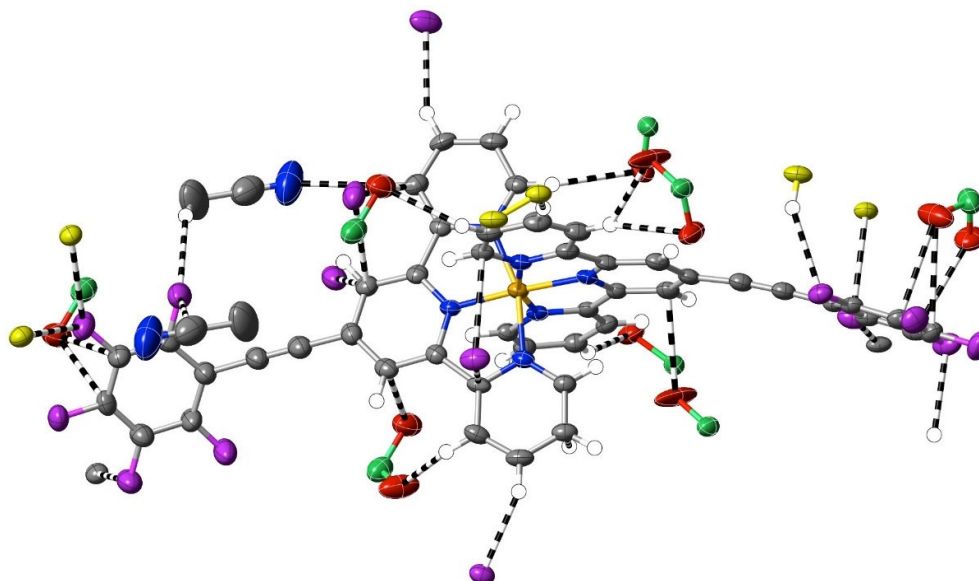
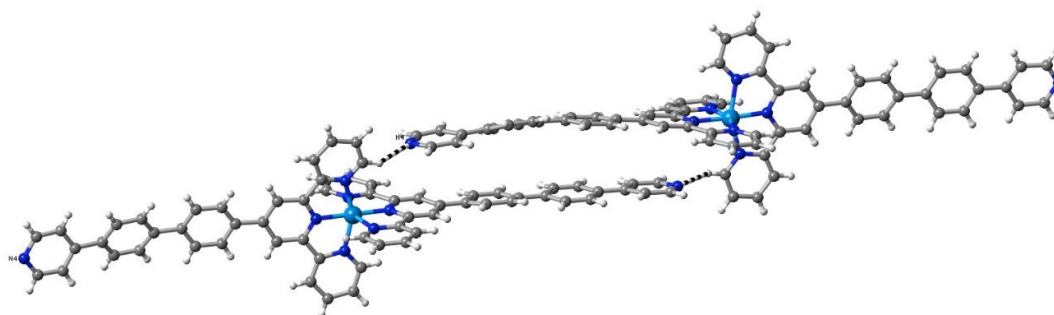


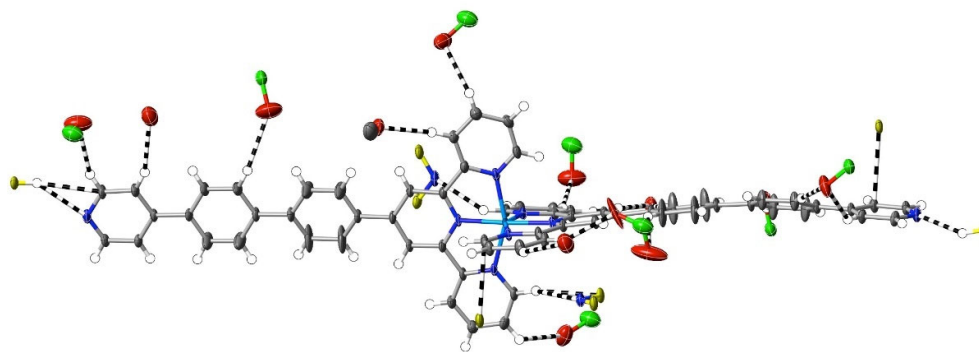
Figure 6. Organofluorine interactions exceeding dispersion in $[\text{Fe}(\text{pfpatpy})_2](\text{ClO}_4)_2 \cdot \text{CH}_3\text{CN} \cdot \text{H}_2\text{O}$, 17.

More subtle consequences of the introduction of a polar substituent in the ligand are seen in the interactions observed in the complexes **18–20** of **pybtpy**. These structures augment those of our earlier work [14] on related $\text{Zn}(\text{II})/\text{pytpy}$ and $\text{Cd}(\text{II})/\text{pybtpy}$ complexes, although that of the $\text{Cu}(\text{II})$ complex **19** is significantly disordered, and its weak interactions cannot be fully analysed. All add to the family of complexes of

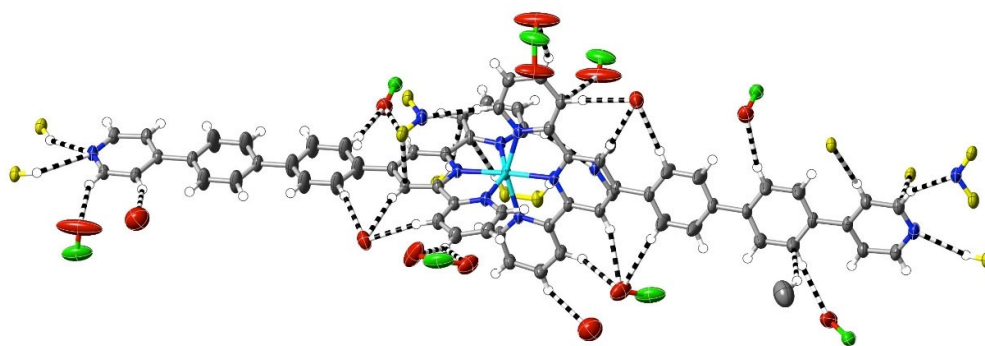
(4-pyridyl)-substituted 2,2':6',2''-terpyridine complexes [71,72], for which a thorough study [72] of complexes of the "parent" ligand 4'-(4-pyridyl)-2,2':6',2''-terpyridine, **pytpy**, has shown not only that the bound ligand may both twist and bow (as observed here) but that the H-bonding capacity of the pyridyl unit has a major influence upon the crystal structure, to the point that it may exclude stacking interactions. In the structures of the extended-ligand complexes $[\text{Zn}(\text{pytpy})_2](\text{ClO}_4)_2 \cdot 2\text{CH}_3\text{OH} \cdot \text{CHCl}_3$ and $[\text{Cd}(\text{pybtpy})_2](\text{ClO}_4)_2 \cdot \text{DMF} \cdot 2.8\text{H}_2\text{O}$ [14], various units with aromatic stacking are apparent, as they are in complexes **18–20**. As is usual with such arrays, any interactions appear to be largely dispersive in nature, but examination of the interactions exceeding dispersion reveals some interesting changes in the pyridine-N interactions as a function of the substituent chain length as it passes from 4-pyridyl through 4-pyridyl-phenyl to 4-pyridyl-biphenyl. Thus, in the bis(ligand) complexes of Fe(II), Ni(II) and Ru(II) with **pytpy** [72], one pyridine-N forms a "classical" H-bond with methanol, and the other, a "non-classical" bond with HC from a separate complex unit, while in $[\text{Zn}(\text{pytpy})_2] \cdot 2\text{CH}_3\text{OH} \cdot \text{CHCl}_3$ [14], both pyridine-N atoms form H-bonds with methanol, but one also forms a bond with HC, and in $[\text{Cd}(\text{pybtpy})_2](\text{ClO}_4)_2 \cdot \text{DMF} \cdot 2.8\text{H}_2\text{O}$ [14] and complexes **18–20**, both pyridine-N atoms form N-HC bonds only. In the polymeric chains involving the stacking of the 4' substituents in the **pybtpy** complexes, these double interactions result in the 4-pyridylbiphenyl units being much closer to planar and lying closer to parallel with their pair than is the case in the otherwise rather similar structures of complexes of the **tptpy** and **papatpy** ligands (Figure 7).



(a) $[\text{Ni}(\text{pybtpy})_2](\text{ClO}_4)_2 \cdot 2\text{DMF} \cdot \text{H}_2\text{O}$, **18**.



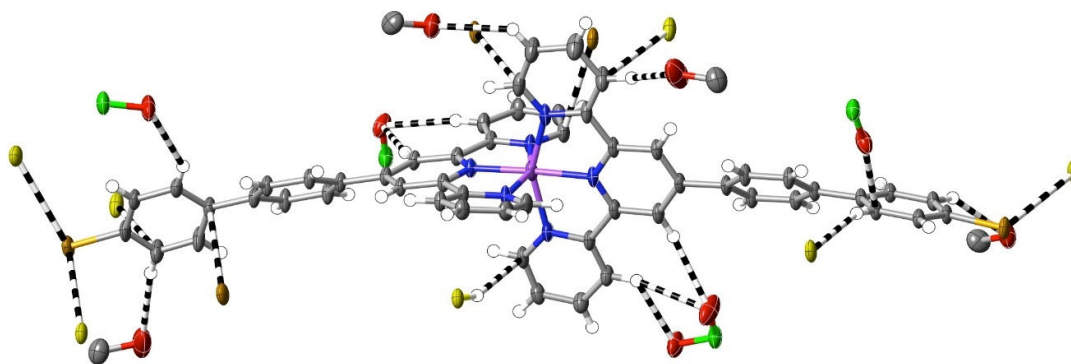
(b) $[\text{Ni}(\text{pybtpy})_2](\text{ClO}_4)_2 \cdot 2\text{DMF} \cdot \text{H}_2\text{O}$, **19**.



(c) $[\text{Zn}(\text{pybptpy})_2](\text{ClO}_4)_2 \cdot 2\text{DMF} \cdot \text{H}_2\text{O}$, 20.

Figure 7. Interactions exceeding dispersion in complexes of **pybptpy**, showing, (a) in the Ni(II) complex as an example, a partial view of the stacking, which appears to be reinforced by N-HC interactions, and (b–c) the full range of cation interactions in the Ni(II) and Zn(II) complexes.

An alternative means of introducing polarity in the same sense as that induced by the pyridine-N of **pybptpy** complexes is seen in the complexes **21–24** of **Brbptpy** with Co(II), Ni(II), Cu(II) and Ru(II). Their structures add to those of Zn(II) and Cd(II) previously described [35], creating another small family of M(II) complexes of the one 2,2':6',2''-terpyridine derivative. The presence of a bromo-substituent raises the prospect of “halogen bonding” [73], but only in the structures of the Ni(II) and Ru(II) complexes is there any evidence for such interactions, and regardless of their nature, interactions of the bromine atoms do not result in any obvious restriction of the twisting of the biphenyl tails. There does appear to be a difference in the interactions beyond dispersion when the first-row transition metal complexes are compared with those of the second-row, with C··C and CH··C interactions being much more prominent for the former and CH··O interactions (involving the counteranions) being almost completely dominant in $[\text{Cd}(\text{Brbptpy})_2](\text{ClO}_4)_2 \cdot \text{CH}_3\text{CN}$, though of course, the number of examples available for comparison is rather small (Figure 8). In no case here is there evidence of nucleophile interaction with C-atoms bound to N.



(a) $[\text{Cu}(\text{Brbptpy})_2](\text{ClO}_4)_2 \cdot 2\text{CH}_3\text{OH}$, 23.

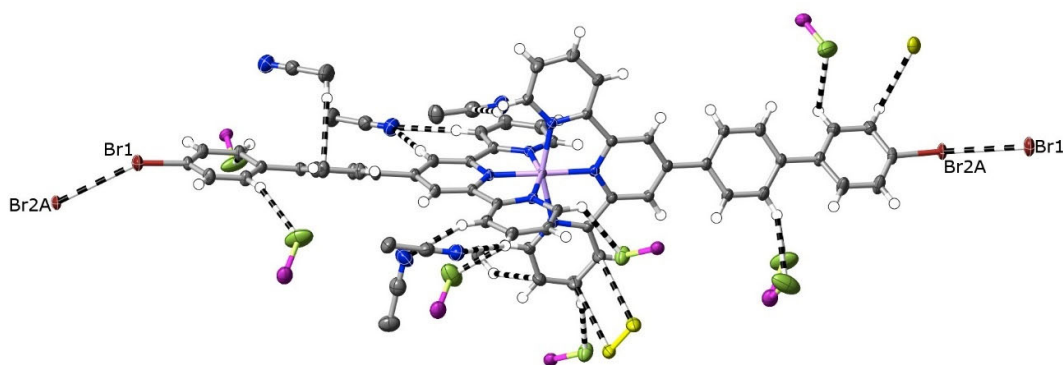
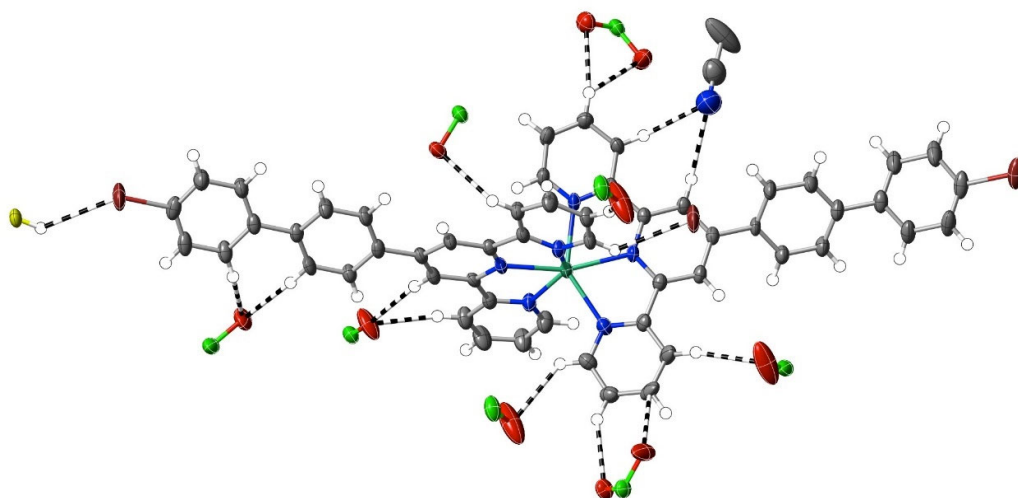
(b) $[\text{Ru}(\text{Brbptpy})_2](\text{PF}_6)_2 \cdot 3\text{CH}_3\text{CN}$, 24.(c) $[\text{Cd}(\text{Brbptpy})_2](\text{ClO}_4)_2 \cdot \text{CH}_3\text{CN}$ [35].

Figure 8. A comparison of interactions beyond dispersion in complexes of first- and second-row transition metal(II) ion complexes of **Brbptpy**.

Adding an ethoxycarbonyl group as the terminus of a 4'-polyphenyl tail introduces an entity with more than one interaction site and possibly capable of directional interactions. Interactions beyond dispersion of the ethoxycarbonyl groups in the complexes $[\text{Ni}(\text{ebptpy})_2](\text{ClO}_4)_2 \cdot 3\text{DMF}$ (25), $[\text{Cu}(\text{ebptpy})_2](\text{ClO}_4)_2 \cdot \text{CH}_3\text{CN}$ (26) and $[\text{Zn}(\text{etptpy})_2](\text{ClO}_4)_2 \cdot 2\text{DMF} \cdot \text{H}_2\text{O}$ (27) are not, however, unusually prominent compared to others such as those involving the counteranions, and the more significant aspect of the structures is the evidence they provide for the importance of dispersive interactions in the arrays adopted by the terpyridine substituents. All three structures are layered, and within the layers, the full interactions are complicated, but in each, it is possible to identify pairs of cations where the substituent tails are in close proximity. In the **ebptpy** complexes, the tails are twisted such that the phenyl rings of adjacent cations are in arrays closer to edge to face rather than face to face, but in the **etptpy** complex, the greater extent of the aromatic tail is reflected in arrays where there is relatively slight twisting, and the three rings of each cation tail are in close-to-parallel (face-to-face) alignment with three of an adjacent cation (Figure 9). There is, nonetheless, only one C–C interaction ($\text{C}28 \dots \text{C}54^i$; $i = 1.5 + x, 1.5 - y, 1 + z$; $3.313(3) \text{ \AA}$) exceeding dispersion occurring between the three pairs of rings, meaning that dispersion alone is clearly the dominant factor.

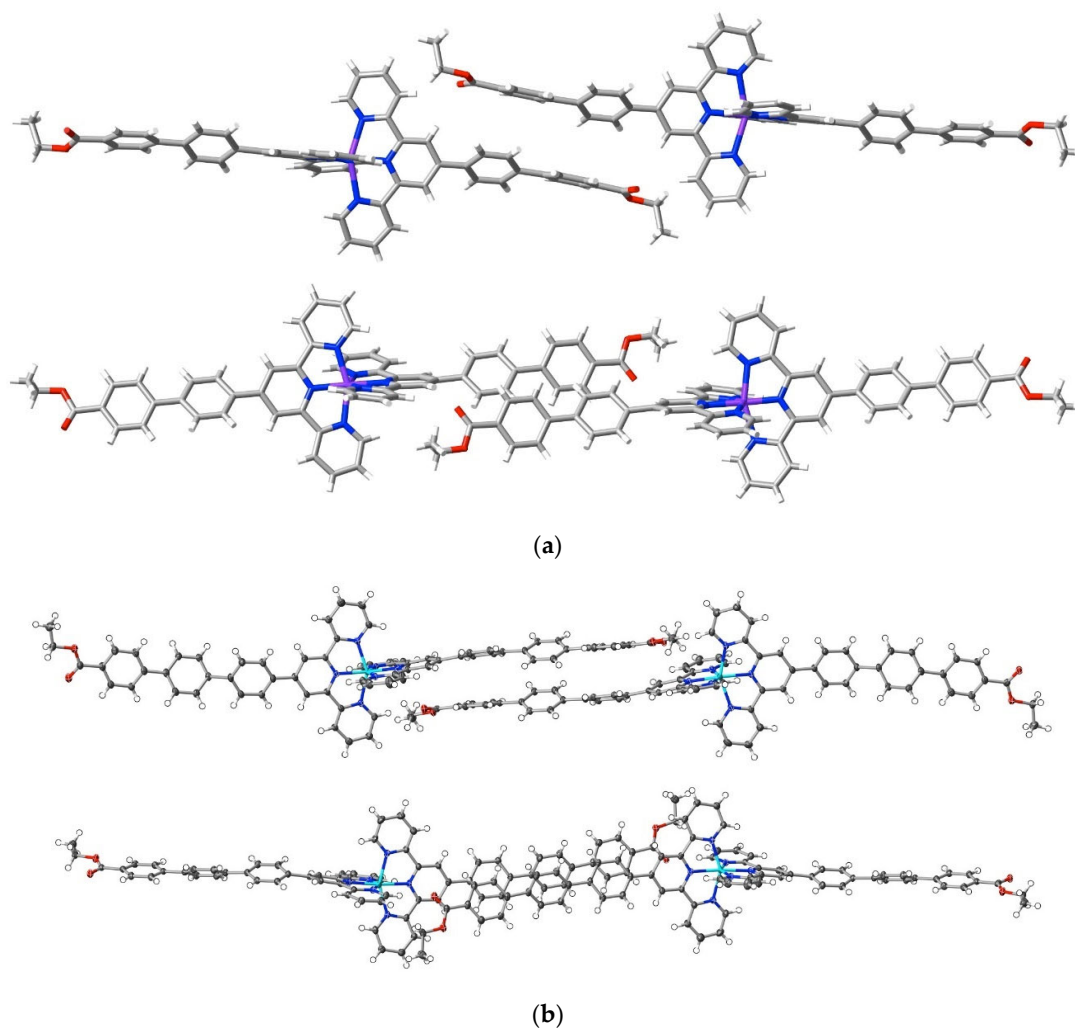
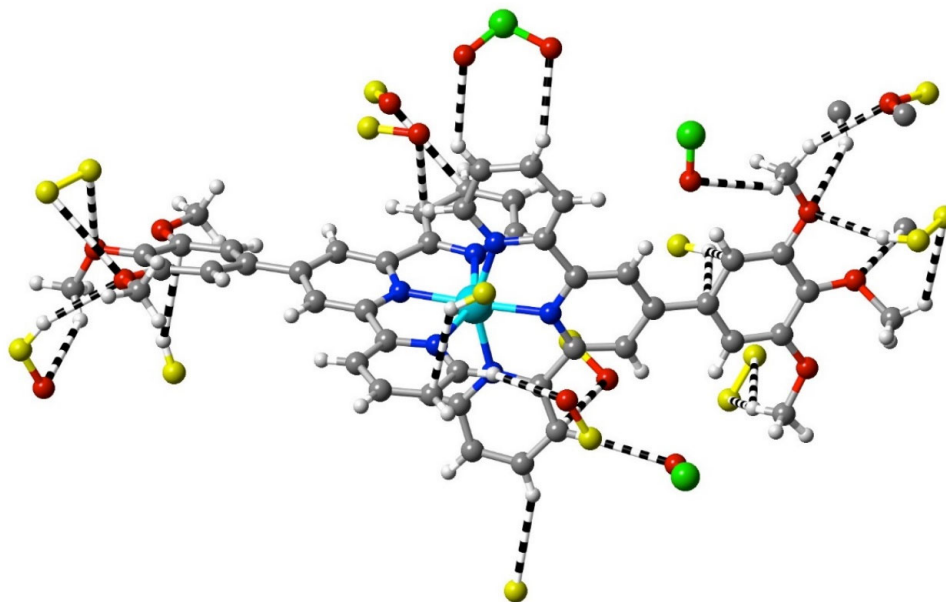


Figure 9. Effect of polyphenyl chain length on stacking arrays in complexes of ethoxycarbonylphenyl-substituted terpyridine complexes. Orthogonal views of proximal arms in (a) $[\text{Cu}(\text{ebtpy})_2](\text{ClO}_4)_2 \cdot \text{CH}_3\text{CN}$, **26**, and (b) $[\text{Zn}(\text{etptpy})_2](\text{ClO}_4)_2 \cdot 2\text{DMF} \cdot \text{H}_2\text{O}$, **27**.

The complexes **28–34** all contain alkoxy-functionalised terpyridine ligands, $[\text{Fe}(\text{bzOtpy})_2](\text{ClO}_4)_2$ (**28**) and $[\text{Ni}(\text{bzOtpy})_2](\text{ClO}_4)_2$ (**29**) being additions to the fairly numerous known family [36,64,74], where the alkoxy group is attached directly to the 4' position of 2,2':6',2''-terpyridine. The Hirshfeld surfaces (Figure S4) obtained for the structures of **28** and **29** show marked differences in the number of interactions beyond dispersion, with, in particular, a complete absence of apparent C··C interactions in **29**. Such loss can be explained as arising from the nearly 200 K difference in the temperatures (**28**, 100 K; **29**, 296 K) at which the structures were determined, with the enhanced vibrational motion at the higher temperature leading to some washing out of the difference between dispersion and other weak interactions. Similar differences have been observed for Co(II) complexes studied in their low-spin and high-spin forms, necessarily at quite different temperatures [37], and the Hirshfeld surface for the cation present in the structure of the Zn(II) complex of the homologous ligand 4'-(4-benzoyloxyphenyl)-2,2':6',2''-terpyridine determined at 291 K [75] also shows little evidence of interactions exceeding dispersion. In **28**, interactions beyond the dispersion of the cation are multiple and various, and CH··C or C··C interactions are not limited to only one close pair. Even a cursory inspection of the Hirshfeld surfaces (Figure S5; all for low-temperature determinations) of **28** and the Co(II) and Cu(II) complexes of the triply methoxylated ligand

4'-(1,2,3-trimethoxy-5-phenyl)-2,2':6',2''-terpyridine, **tmbzOtpy** [36], shows that the introduction of the methoxyl substituents quite dramatically modifies all interactions beyond the dispersion of the cations, further supporting the contention that these interactions are generally a reflection of equilibria involving multivariate influences.

The structures of the complexes **31–34** provide additions to those related examples also concerning terpyridines with trimethoxyphenyl (gallate) substituents previously considered [36] in relation to their possible use as precursors to mesogenic species. While in the protonated **tmtpy** ligand (structure **30**), all the interactions beyond dispersion with the perchlorate anions are of the CH···O type, in the Zn(II) complex **31** (Figure 10a), there are two methoxyl-O···C contacts (C12···O2ⁱ 3.20(6) Å; C13···O1ⁱ 3.19(6); $i = x + 0.5, 2 - y, 3 - z$), perhaps indicative of the greater nucleophilicity of methoxyl-O compared to perchlorate-O, although neither C12 nor C13 is bound directly to coordinated N. In all the three complexes **32–34** (Figure 10b–d), however, there are methoxyl-O contacts with C bound to N, and an explanation for this unexpectedly great activity of methoxyl-O may be that it is induced by a multiplicity of other interactions exceeding the dispersion of the 1,2,3-trimethoxyphenyl units. As noted for the earlier examples, these structures display clear stacking arrays of the trimethoxyphenyl rings with terpyridine units, but the interactions beyond dispersion within the stacked assemblies are of CH···O or C···O types only, not C···C.



(a) $[\text{Zn}(\text{tmtpy})_2](\text{ClO}_4)_2 \cdot \text{CH}_3\text{CN}$, **31**.

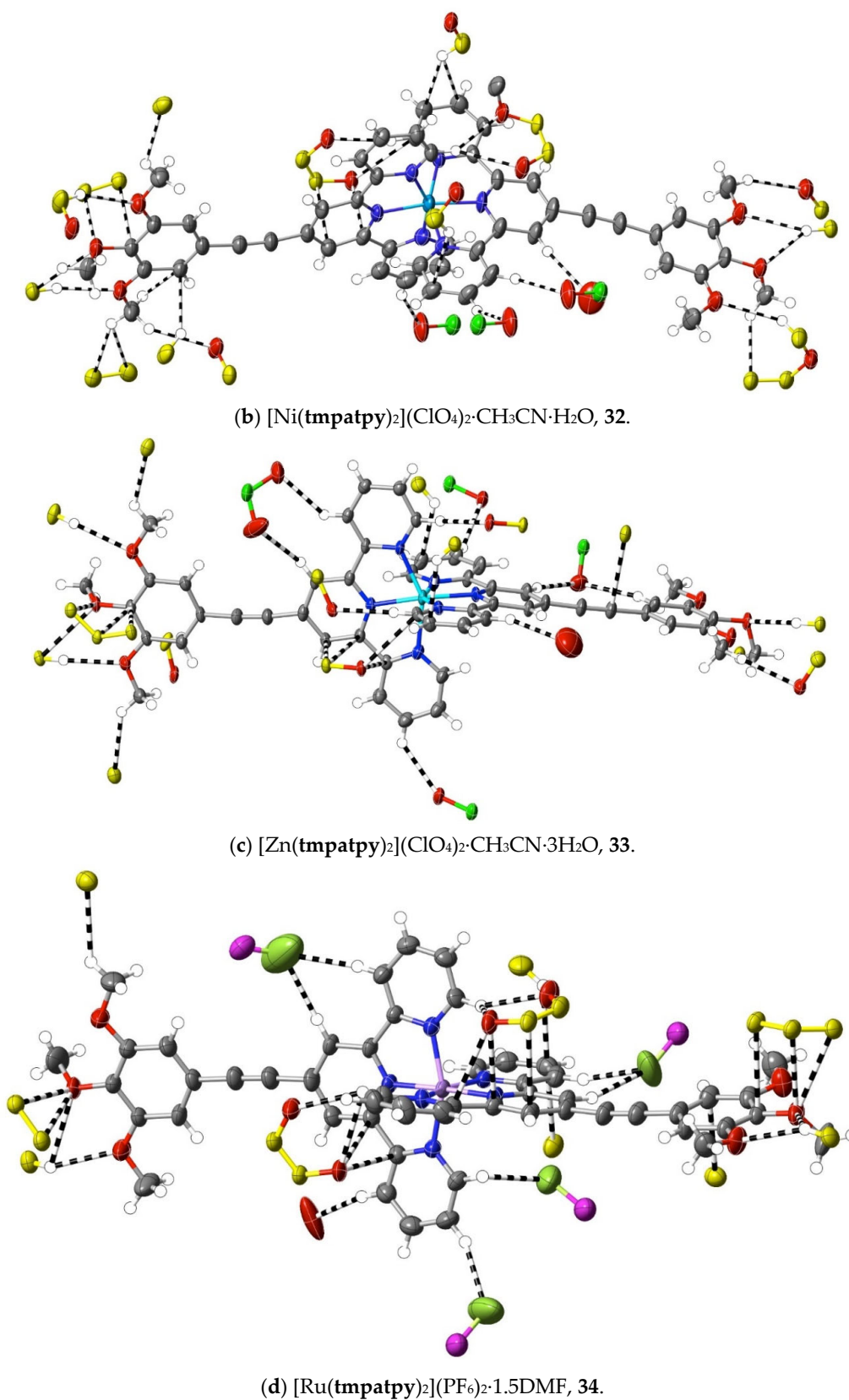


Figure 10. Interactions beyond dispersion of complex cations incorporating trimethoxyphenyl-substituted 2,2':6',2''-terpyridine ligands.

5. Conclusions

Given that the structures reported herein, even with the addition of various known relatives in the literature, represent only a small fraction of the total number known (5200 for terpyridines generally and 1798 for complexes of 4'-substituted terpyridines in the Cambridge Structural Database [76]), it would be unwise to draw general conclusions from what has been seen in the Hirshfeld surface analysis conducted. Ideally, comparisons might be better made of isostructural species with common counteranions for structures determined at the same low temperature, but given the vagaries of growing crystals suitable for structure determination, this is probably not a feasible task, at least as the basis of an extensive investigation. What can be said from the present observations is that a consideration of the interactions exceeding dispersion alone in the crystals of terpyridine complexes offers a rather complicated description of any structure that is not readily related, in an experimental sense, to the dispersive interactions, which may be dominant in stacked arrays of aromatic units. It is, of course, unremarkable that cation-anion interactions appear as major influences exceeding dispersion, but they are clearly in competition with other interactions, resulting in balance points that vary considerably, even for closely related species. The possibility that weak interactions exceeding dispersion may reflect ligand polarisation due to coordination—specifically, that with coordinated poly(aza-aromatic) ligands, carbon bound to nitrogen becomes significantly more electrophilic than in the free ligand—has some support in what is seen with highly charged (V(V) and U(VI)) cations but needs further investigation, perhaps through efforts to crystallise the complexes as simple hydroxide or fluoride salts. In relation, generally, to how the properties of any given complex might be influenced by its supramolecular (weak) interactions, it must be noted that the structures studied reveal the importance of, for example, non-classical CH interactions but show little involvement of ethynyl units, perhaps only because of the limited natures of other species (anions and solvents) present within the structures, making this an issue also needing further study.

Supplementary Materials: The following are available online at www.mdpi.com/3/1/16/s1. Figure S1: One cation of the structure of $[\text{VO}_2(\text{btpy})]\text{ClO}_4$, **1**, showing its environment of other cations involved in C–C and CH–C interactions beyond dispersion with that cation. For clarity, only the ligand units of the surrounding cations involved in the interactions are shown (in yellow) and no H-atoms other than those involved in interactions are shown.; Figure S2: O–C contacts indicative of interactions beyond dispersion in stacked uranyl ion complexes. For clarity, stick representations are used and H-atoms are not shown.; Figure S3: Interactions beyond dispersion for cations in complexes of 4'-biphenyl-2,2':6',2''-terpyridine (**btpy**). Structures reported in reference [63]. Colour coding as for Figure 1; Figure S4: Hirshfeld surfaces, d_{norm} representations in non-transparent mode to render more obvious the red regions indicative of interactions beyond dispersion, for (a) $[\text{Fe}(\text{bzOtpy})_2](\text{ClO}_4)_2$, **28**, and (b) $[\text{Ni}(\text{bzOtpy})_2](\text{ClO}_4)_2$, **29**, along with representations of the full interactions of the cations; Figure S5: Hirshfeld surface diagrams, d_{norm} representations, transparent mode, as obtained with CrystalExplorer for complexes of benzyloxy-substituted terpyridine ligands with or without methoxyl functionalisation; Table S1: Volume of voids per unit cell, number of electrons per void, and possible solvent molecules occupying the voids, as deduced from SQUEEZE results.

Author Contributions: Conceptualisation, Y.H.L., J.H. and Y.K.; methodology, Y.H.L., Y.K. and J.H.; supervision, J.H., Y.K. and S.H.; funding acquisition, Y.K. and S.H.; synthesis, Y.H.L., J.Y.K., S.K., H.O. and M.H.; crystallography and data analysis, P.T., Y.H.L. and J.H.; writing, J.H. All authors have read and agreed to the published version of the manuscript.

Funding: Partial funding for this work was provided by a KAKENHI Grant-in-Aid for Scientific Research (A) JP17H01200.

Data Availability Statement: CCDC depositions 2055133-2055135, 2055137-2055142, 2055148-2055161 and 2055219-2055228 contain the supplementary crystallographic data for this paper. These data can be obtained free of charge via www.ccdc.cam.ac.uk/data_request/cif, or by e-mailing data_request@ccdc.cam.ac.uk, or by contacting The Cambridge Crystallographic Data Centre, 12 Union Road, Cambridge CB2 1EZ, UK; Fax: +44-12-2333-6033.

Acknowledgments: Shinya Hayami is grateful for the support provided by the KAKENHI Grant-in-Aid for Scientific Research. Jack Harrowfield thanks Jean-Marie Lehn for the privilege of continuing, after retirement, to work within his group.

Conflicts of Interest: The authors declare no conflict of interest.

References

1. Hofmeier, H.; Schubert, U.S. Recent developments in the supramolecular chemistry of terpyridine–metal complexes. *Chem. Soc. Rev.* **2004**, *33*, 373–399.
2. Schubert, U.S.; Hofmeier, H.; Newkome, G.R. *Modern Terpyridine Chemistry*; Wiley-VCH: Weinheim, Germany, 2006.
3. Constable, E.C. 2,2':6',2"-Terpyridines: From chemical obscurity to common supramolecular motifs. *Chem. Soc. Rev.* **2007**, *36*, 246–253.
4. Constable, E.C.; Housecroft, C.E. 'Simple' Oligopyridine Complexes – Sources of Unexpected Structural Diversity. *Aust. J. Chem.* **2020**, *73*, 390–398.
5. Wild, A.; Winter, A.; Schlütter, F.; Schubert, U.S. Advances in the field of π -conjugated 2,2':6',2"-terpyridines. *Chem. Soc. Rev.* **2011**, *40*, 1459–1511.
6. Winter, A.; Newkome, G.R.; Schubert, U.S. Catalytic Applications of Terpyridines and their Transition Metal Complexes. *ChemCatChem* **2011**, *3*, 1384–1406.
7. Hancock, R.D. The pyridyl group in ligand design for selective metal ion complexation and sensing. *Chem. Soc. Rev.* **2013**, *42*, 1500–1524.
8. Mutai, T.; Satou, H.; Araki, K. Reproducible on–off switching of solid-state luminescence by controlling molecular packing through heat-mode interconversion. *Nat. Mater.* **2005**, *4*, 685–687.
9. Scudder, M.L.; Goodwin, H.A.; Dance, I.G. Crystal supramolecular motifs: two-dimensional grids of terpy embraces in $[ML_2]^2$ complexes (L = terpy or aromatic N_3 -tridentate ligand). *New J. Chem.* **1999**, *23*, 695–705.
10. McMurtrie, J.; Dance, I. Engineering grids of metal complexes: development of the 2D $M(\text{terpy})_2$ embrace motif in crystals. *CrystEngComm* **2005**, *7*, 216–219.
11. Dance, I.G.; Scudder, M.L. Molecules embracing in crystals. *CrystEngComm* **2009**, *11*, 2233–2247.
12. Figgis, B.N.; Kucharski, E.S. Crystal structure of Bis(2,2':6',2"-terpyridyl)cobalt(II) iodide dihydrate at 295 K and at 120 K. *Aust. J. Chem.* **1983**, *36*, 1527–1535.
13. McMurtrie, J.; Dance, I. Alternative metal grid structures formed by $[M(\text{terpy})_2]^{2+}$ and $[M(\text{terpyOH})_2]^{2+}$ complexes with small and large tetrahedral dianions, and by $[Ru(\text{terpy})_2]^0$. *CrystEngComm* **2010**, *12*, 2700–2710.
14. Kubota, E.; Lee, Y.H.; Fuyuhiko, A.; Kawata, S.; Harrowfield, J.M.; Kim, Y.; Hayami, S. Synthesis, structure, and luminescence properties of arylpyridine-substituted terpyridine Zn(II) and Cd(II) complexes. *Polyhedron* **2013**, *52*, 435–441.
15. Janiak, C. A critical account on π – π stacking in metal complexes with aromatic nitrogen-containing ligands. *J. Chem. Soc. Dalton Trans.* **2000**, 3885–3896.
16. Jennings, W.B.; Farrell, B.M.; Malone, J.F. Attractive Intramolecular Edge-to-Face Aromatic Interactions in Flexible Organic Molecules. *Acc. Chem. Res.* **2001**, *34*, 885–894.
17. Waters, M.L. Aromatic interactions in model systems. *Curr. Opin. Chem. Biol.* **2002**, *6*, 736–741.
18. Grimme, S. Do special noncovalent π – π stacking interactions really exist? *Angew. Chem. Int. Ed.* **2008**, *47*, 3430–3434.
19. Ehrlich, S.; Moellmann, J.; Grimme, S. Dispersion-Corrected Density Functional Theory for Aromatic Interactions in Complex Systems. *Acc. Chem. Res.* **2013**, *46*, 916–926.
20. Bloom, J.W.G.; Wheeler, S.E. Taking the Aromaticity out of Aromatic Interactions. *Angew. Chem. Int. Ed.* **2011**, *50*, 7847–7849.
21. Martinez, C.R.; Iverson, B.L. Rethinking the term "pi-stacking". *Chem. Sci.* **2012**, *3*, 2191–2201.
22. Waters, M.L. Aromatic Interactions. *Acc. Chem. Res.* **2013**, *46*, 873.
23. Gavezzotti, A. The "Sceptical Chymist": Intermolecular Doubts and Paradoxes. *CrystEngComm* **2013**, *15*, 4027–4035.
24. Malenov, D.P.; Zaric, S.D. Stacking Interactions between Indenyl Ligands of Transition Metal Complexes: Crystallographic and Density Functional Study. *Cryst. Growth Des.* **2020**, *20*, 4491–4502.
25. Gavezzotti, A. Calculation of Intermolecular Interaction Energies by Direct Numerical Integration over Electron Densities. I. Electrostatic and Polarization Energies in Molecular Crystals. *J. Phys. Chem. B* **2002**, *106*, 4145–4154.
26. Dunitz, J.D.; Gavezzotti, A. Molecular Recognition in Organic Crystals: Directed Intermolecular Bonds or Nonlocalized Bonding? *Angew. Chem. Int. Ed.* **2005**, *44*, 1766–1787.
27. Dunitz, J.D.; Gavezzotti, A. Supramolecular Synthons: Validation and Ranking of Intermolecular Interaction Energies. *Cryst. Growth Des.* **2012**, *12*, 5873–5877.
28. Henry, M. Nonempirical Quantification of Molecular Interactions in Supramolecular Assemblies *ChemPhysChem* **2002**, *3*, 561–569.
29. Spackman, M.A.; Jayatilaka, D. Hirshfeld Surface Analysis. *CrystEngComm* **2009**, *11*, 19–32.
30. Wolff, S.K.; Grimwood, D.J.; McKinnon, J.J.; Turner, M.J.; Jayatilaka, D.; Spackman, M.A. (Eds.) *CrystalExplorer 3.1*; University of Western Australia: Perth, Australia, 2012.
31. Spackman, M.A. Molecules in Crystals. *Phys. Scr.* **2013**, *87*, 048103.
32. McKenzie, C.F.; Spackman, P.R.; Jayatilaka, D.; Spackman, M.A. *CrystalExplorer* model energies and energy frameworks: extension to metal coordination compounds, organic salts, solvates and open-shell systems. *IUCr* **2017**, *4*, 575–587.

33. Lee, Y.H.; Kim, J.Y.; Kim, Y.; Hayami, S.; Shin, J.W.; Harrowfield, J.M.; Stefankiewicz, A.R. Lattice Interactions of Terpyridines and Their Derivatives – Free Terpyridines and Their Protonated Forms. *CrystEngComm* **2016**, *18*, 8059–8071.
34. Lee, Y.H.; Kubota, E.; Fuyuhiko, A.; Kawata, S.; Harrowfield, J.M.; Kim, Y.; Hayami, S. Synthesis, structure and luminescence properties of Cu(II), Zn(II) and Cd(II) complexes with 4'-terphenylterpyridine. *Dalton Trans.* **2012**, *41*, 10825–10831.
35. Lee, Y.H.; Fuyuhiko, A.; Harrowfield, J.M.; Kim, Y.; Sobolev, A.N.; Hayami, S. Quaterphenylterpyridine: synthesis, structure and metal-ion-enhanced charge transfer. *Eur. J. Inorg. Chem.* **2013**, 5862–5870.
36. Lee, Y.H.; Harrowfield, J.M.; Shin, J.W.; Won, M.S.; Rukmini, E.; Hayami, S.; Min, K.S.; Kim, Y. Supramolecular interactions of terpyridine-derived cores of metallomesogen precursors. *Int. J. Mol. Sci.* **2013**, *14*, 20729–20743.
37. Lee, Y.H.; Won, M.S.; Harrowfield, J.M.; Kawata, S.; Hayami, S.; Kim, Y. Spin crossover in Co(II) metallorods – replacing aliphatic tails by aromatic. *Dalton Trans.* **2013**, *42*, 11507–11521.
38. Janiak, C. Engineering coordination polymers towards applications. *Dalton Trans.* **2003**, 2781–2804.
39. Wu, M.; Mao, J.; Guo, J.; Ji, S. The Use of a Bifunctional Copper Catalyst in the Cross-Coupling Reactions of Aryl and Heteroaryl Halides with Terminal Alkynes. *Eur. J. Org. Chem.* **2008**, 4050–4054.
40. Constable, E.C.; Ward, M.D. Synthesis and co-ordination behaviour of 6',6''-bis(2-pyridyl)-2,2':4,4'':2'',2'''-quaterpyridine; 'back-to-back' 2,2':6',2''-terpyridine. *J. Chem. Soc. Dalton Trans.* **1990**, 1405–1409.
41. Potts, K.T.; Konwar, D. Synthesis of 4'-vinyl-2,2':6',2''-terpyridine. *J. Org. Chem.* **1991**, *56*, 4815–4816.
42. Grosshenny, V.; Romero, F.; Ziesel, R. Construction of Preorganized Polytopic Ligands via Palladium-Promoted Cross-Coupling Reactions. *J. Org. Chem.* **1997**, *62*, 1491–1500.
43. Alcock, N.W.; Barker, P.R.; Haider, J.M.; Hannon, M.J.; Painting, C.L.; Pikramenou, Z.; Plummer, E.A.; Rissanen, K.; Saarenketo, P. Red and blue luminescent metallo-supramolecular coordination polymers assembled through π - π interactions. *J. Chem. Soc. Dalton Trans.* **2000**, 1447–1461.
44. Collin, J.-P.; Guillerez, S.; Sauvage, J.-P.; Barigelletti, F.; De Cola, L.; Flamigni, L.; Balzani, V. Photoinduced processes in dyads and triads containing a ruthenium(II)-bis(terpyridine) photosensitizer covalently linked to electron donor and acceptor groups. *Inorg. Chem.* **1991**, *30*, 4230–4238.
45. Tu, S.; Jia, R.; Jiang, B.; Zhang, J.; Zhang, Y.; Yao, C.; Ji, S. Kröhnke reaction in aqueous media: one-pot clean synthesis of 4'-aryl-2,2':6',2''-terpyridines. *Tetrahedron* **2007**, *63*, 381–388.
46. Benniston, A.C.; Chapman, G.; Harriman, A.; Mehrabi, M.; Sams, C.A. Electron Delocalization in a Ruthenium(II) Bis(2,2':6',2''-terpyridyl) Complex. *Inorg. Chem.* **2004**, *43*, 4227–4233.
47. Muro, M.L.; Castellano, F.N. Room temperature photoluminescence from [Pt(4'-CCR-tpy)Cl]⁺ complexes. *Dalton Trans.* **2007**, 4659–4665.
48. Du, P.; Schneider, J.; Brennessel, W.W.; Eisenberg, R. Synthesis and Structural Characterization of a New Vapochromic Pt(II) Complex Based on the 1-Terpyridyl-2,3,4,5,6-pentaphenylbenzene (TPPPB) Ligand. *Inorg. Chem.* **2008**, *47*, 69–77.
49. Popović, Z.; Busby, M.; Huber, S.; Calzaferri, G.; De Cola, L. Assembling Micro Crystals through Cooperative Coordinative Interactions. *Angew. Chem. Int. Ed.* **2007**, *46*, 8898–8902.
50. Constable, E.C.; Cargill-Thompson, A.M.W.; Tocher, D.A.; Daniels, M.A.M. Synthesis, characterisation and spectroscopic properties of ruthenium(II)-2,2':6',2''-terpyridine coordination triads. X-Ray structures of 4'-(N,N-dimethylamino)-2,2':6',2''-terpyridine and bis(4'-(N,N-dimethylamino)-2,2':6',2''-terpyridine)ruthenium(II) hexafluorophosphate acetonitrile solvate. *New J. Chem.* **1992**, *16*, 855–867.
51. Arvai, A.J.; Nielsen, C. *ADSC Quantum-210 ADX Program*; Area Detector System Corporation: Poway, CA, USA, 1983.
52. Otwinowski, Z.; Minor, W. Processing of X-ray diffraction data collected in oscillation mode. *Methods Enzymol.* **1997**, *276*, 307–326.
53. Sheldrick, G.M. Crystal Structure Refinement with SHELXL. *Acta Cryst.* **2015**, *C71*, 3–8.
54. Spek, A.L. PLATON SQUEEZE: a tool for the calculation of the disordered solvent contribution to the calculated structure factors. *Acta Cryst.* **2015**, *C71*, 9–18.
55. *CrystalMaker 8.7*; CrystalMaker Software Ltd.: Woodstock, UK, 2014.
56. Florio, P.; Coghlan, C.J.; Lin, C.-P.; Saito, K.; Campi, E.M.; Jackson, W.R.; Hearn, M.T.W. Isolation and Structure of a Hydrogen-bonded 2,2':6',2''-Terpyridin-4'-one Acetic Acid Adduct. *Aust. J. Chem.* **2014**, *67*, 651–656.
57. Murguly, E.; Norsten, T.B.; Branda, N. Tautomerism of 4-hydroxyterpyridine in the solid, solution and gas phases: an X-ray, FT-IR and NMR study. *J. Chem. Soc. Perkin Trans. II* **1999**, 2789–2794.
58. Fallahpour, R.-A.; Constable, E.C. Novel synthesis of substituted 4'-hydroxy-2,2':6',2''-terpyridines. *J. Chem. Soc., Perkin Trans. I* **1997**, 2263–2264.
59. Liu, Y.; Hong, X.; Lu, W.-G.; Lai, S. A vanadium(V) terpyridine complex: synthesis, characterization, cytotoxicity in vitro and induction of apoptosis in cancer cells. *Transition Met. Chem.* **2017**, *42*, 459–467.
60. Thangavelu, S.G.; Andrews, M.B.; Pope, S.J.A.; Cahill, C.L. Synthesis, Structures, and Luminescent Properties of Uranyl Terpyridine Aromatic Carboxylate Coordination Polymers. *Inorg. Chem.* **2013**, *52*, 2060–2069.
61. Carter, K.P.; Kalaj, M.; Cahill, C.L. Probing the Influence of N-Donor Capping Ligands on Supramolecular Assembly in Molecular Uranyl Materials. *Eur. J. Inorg. Chem.* **2016**, 126–137.
62. Lyczko, K.; Steczek, L. Crystal structure of a hydroxo-bridged dimeric uranyl complex with a 2,2':6',2''-terpyridine ligand. *J. Struct. Chem.* **2017**, *58*, 102–106.
63. Gomez, G.E.; Ridenour, J.A.; Byrne, N.M.; Shevchenko, A.P.; Cahill, C.L. Novel Heterometallic Uranyl-Transition Metal Materials: Structure, Topology, and Solid State Photoluminescence Properties. *Inorg. Chem.* **2019**, *58*, 7243–7254.

64. Junk, P.C.; Kepert, C.J.; Semenova, L.I.; Skelton, B.W.; White, A.H. The Structural Systematics of Protonation of Some Important Nitrogen-base Ligands. I. Some Univalent Anion Salts of Doubly Protonated 2, 2':6', 2''-Terpyridyl. *Zeit. Anorg. Allg. Chem.* **2006**, *632*, 1293–1302.
65. Maslen, E.N.; Raston, C.L.; White, A.H. Crystal structure of bis(2,2':6',2''-terpyridyl)cobalt(II) bromide trihydrate. *J. Chem. Soc., Dalton Trans.* **1974**, 1803–1807.
66. Nielsen, P.; Toftlund, H.; Bond, A.D.; Boas, J.F.; Pillbrow, J.R.; Hansen, G.R.; Noble, C.; Riley, M.J.; Neville, S.M.; Moubaraki, B.; Murray, K. S. Systematic study of spin crossover and structure in [Co(terpyRX)₂](Y)₂ systems (terpyRX = 4'-alkoxy-2,2':6',2''-terpyridine, X = 4, 8, 12, Y = BF₄⁻, ClO₄⁻, PF₆⁻, BPh₄⁻). *Inorg. Chem.* **2009**, *48*, 7033–7047.
67. Figgis, B.N.; Kucharski, E.S.; White, A.H. Crystal structure of Bis(2,2':6',2''-terpyridyl)cobalt(III) chloride. *Aust. J. Chem.* **1983**, *36*, 1563–1571.
68. Paul, J.; Spey, S.; Adams, H.; Thomas, J.A. Synthesis and structure of rhodium complexes containing extended terpyridyl ligands. *Inorg. Chim. Acta* **2004**, *357*, 2827–2832.
69. Wickramasinghe, W.A.; Bird, P.H.; Serpone, N. Interligand pockets in polypyridyl complexes. Crystal and molecular structure of the bis(terpyridyl)chromium(III) cation. *Inorg. Chem.* **1982**, *21*, 2694–2698.
70. Sugihara, H.; Hiratani, K. 1,10-phenanthroline derivatives as ionophores for alkali metal ions. *Coord. Chem. Rev.* **1996**, *148*, 285–299.
71. Granifo, J.; Garland, M.T.; Baggio, R. Hydrogen bonding and π -stacking interactions in the zipper-like supramolecular structure of the monomeric cadmium(II) complex [Cd(pyterpy)(H₂O)(NO₃)₂] (pyterpy = 4'-(4-pyridyl)-2,2':6',2''-terpyridine). *Inorg. Chem. Commun.* **2004**, *7*, 77–81.
72. Beves, J.E.; Bray, D.J.; Clegg, J.K.; Constable, E.C.; Housecroft, C.E.; Jolliffe, K.A.; Kepert, C.J.; Lindoy, L.F.; Neuburger, M.; Price, D.J.; Schaffner, S.; Schaper, F. Expanding the 4,4'-bipyridine ligand: Structural variation in {M(pytpy)₂}²⁺ complexes (pytpy = 4'-(4-pyridyl)-2,2':6',2''-terpyridine, M = Fe, Ni, Ru) and assembly of the hydrogen-bonded, one-dimensional polymer {[Ru(pytpy)(Hpytpy)]_n}³ⁿ⁺. *Inorg. Chim. Acta* **2008**, *361*, 2582–2590.
73. Metrangolo, P.; Resnati, G. Halogen Bonding: A Paradigm in Supramolecular Chemistry. *Chem. Eur. J.* **2001**, *7*, 2511–2519.
74. Constable, E.C.; Harris, K.; Housecroft, C.E.; Neuburger, M.; Zampese, J.A. Turning [M(tpy)₂]ⁿ⁺ embraces and CH \cdots π interactions on and off in homoleptic cobalt(II) and cobalt(III) bis(2,2':6',2''-terpyridine) complexes. *CrystEngComm* **2010**, *12*, 2949–2961.
75. Li, W.; Lu, Z.G. Diacetato{4'-[4-(benzyloxy)phenyl]-2,2':6',2''-terpyridine}zinc(II). *Acta Cryst.* **2009**, *E65*, m1672.
76. Groom, C.R.; Bruno, I.J.; Lightfoot, M.P.; Ward, S.C. The Cambridge Structural Database. *Acta Cryst.* **2016**, *B72*, 171–179.